Dispersion-Tailored Few-Mode Fibers: A Versatile Platform for In-Fiber Photonic Devices

Siddharth Ramachandran, *Member, IEEE*

***Abstract*—In-fiber devices enable a vast array of critical photonic functions ranging from signal conditioning (amplification, dispersion control) to network management (add/drop multiplexers, optical monitoring). These devices have become mainstays of fiber-optic communication systems because they provide the advantages of low loss, polarization insensitivity, high reliability, and compatibility with the transmission line. The majority of fiber devices reported to date are obtained by doping, designing, or writing gratings in the core of a single-mode fiber (SMF). Thus, these devices use the fiber only as a platform for propagating light—the device effect itself is due to some extraneously introduced material or structure (dopants for amplification, gratings for phase matching, etc.)**

There exists another, relatively less explored degree of freedom afforded by fibers—the ability to copropagate more than one mode. Each mode may have a uniquely defined modal dispersion and propagation characteristic. In this paper, we will describe the variety of fiber devices enabled by few-mode fibers—fibers that typically support two to four modes with suitably tailored dispersive properties. We will show that the unique dispersive properties of various modes, in conjunction with the ability to couple between them with gratings, leads to devices that offer novel solutions for dispersion compensation, spectral shaping, and polarization control, to name a few.

***Index Terms*—Attenuators, bandpass filters, bit error rate (BER), broadband, dispersion compensation, effective area, fiber design, grating packaging, grating reliability, grating stability, gratings, group delay (GD), long-period fiber gratings (LPGs), microbends, mode conversion, noise figure, optical fiber dispersion, optical nonlinearities, optical phase matching, optical signal to noise, optical switch, optical transmission systems, polarization-dependent loss (PDL), polarizers, sensors, strain sensors, temperature sensors, tunable dispersion compensation, tunable gratings, variable optical attenuators (VOA).**

I. Introduction

IN-FIBER devices have attracted a lot of attention since the invention of the erbium-doped fiber amplifier (EDFA). These devices have become mainstays in fiber-optic communication systems, because they provide the advantages of low loss, polarization insensitivity, high reliability, and compatibility with the transmission line. They have found several applications, ranging from signal conditioning (amplification, dispersion control, etc.) to network management (add/drop multiplexing, optical monitoring, etc.). Fiber-waveguide engineering has enabled dispersion control of optical signals, and dispersion-compensating fibers (DCF) are the preferred commercially deployed dispersion-management devices in transmission systems today [1]. Fiber-based resonant couplers, fabricated by either fusing fibers or by inducing periodic perturbations (gratings within the core of a fiber), have become the device schematic of choice for a variety of functions, such as signal or pump de/multiplexing [2], optical monitoring, tunable dispersion compensation [3], and static [4], [5], as well as dynamic, spectral shaping [6], [7], to name a few.

Common to several fiber devices is the single-mode fiber (SMF), which serves as a platform to propagate the signal. Light propagates in the fundamental mode of the fiber, and the device effect itself is due to some extraneously introduced material or structure (dopants for amplification, gratings for phase matching, etc.). In this respect, they are similar to bulk optic devices.

There exists another, relatively less explored degree of freedom afforded by fibers—the ability to copropagate more than one mode—in so-called few-mode fibers. These fibers can be manufactured by standard processing techniques used to realize commercial transmission fibers and, thus, offer several of the economies of scale offered by fiber devices. Each mode may be designed to have a uniquely defined modal dispersion and propagation characteristic. Since a large majority of fiber devices, such as in-fiber gratings, fused couplers, and DCFs, primarily exploit changes in the phase of light as it propagates through the fiber device, a few-mode fiber guiding several modes with different propagation constants both expands the design space accessible to existing devices and facilitates novel device effects.

This paper will review the variety of fiber devices enabled by few-mode fibers—fibers that typically support two to four modes with suitably tailored dispersive properties. Table I summarizes the variety of applications spaces in the field of photonics that these devices have impacted. Few-mode fiber devices demonstrated to date fall in three general classes: 1) novel device effects that are unique to few-mode fiber devices, such as dispersionless filters and polarization-dependent loss (PDL) controllers; 2) applications that provide enhanced performance in comparison to conventional fiber devices, thus providing strong competition to existing devices, such as higher order mode dispersion-compensating modules (HOM-DCM), and very low-loss and low-cost variable optical attenuators (VOA); and 3) devices offering novel functionalities that can be potentially disruptive to current optical-networking architectures, such as wavelength-continuous broadband tunable dispersion compensators (TDCs).

The fundamental building block for few-mode fiber devices is a static or tunable mode converter, which allows the shuffling of the optical signal between various modes of the fiber. All

Manuscript received December 23, 2003; revised February 25, 2005.

The author is with the OFS Laboratories, Somerset, NJ 08873 USA (e-mail: sidr@ieee.org).

Digital Object Identifier 10.1109/JLT.2005.855874

TABLE I
PHOTONIC DEVICES WITH FEW-MODE FIBERS. APPLICATION SPACE COVERED BY PHOTONIC DEVICES IN FEW-MODE FIBERS. THIS VERSATILE PLATFORM HAS ENABLED DEVICE APPLICATIONS IN A LARGE NUMBER OF AREAS IN PHOTONICS

Dispersion control	Signal power management	Switching/ Routing	Polarisation	Sensing
Higher-order-mode Dispersion Compensation • Lower nonlinearities • Longer transmission distance	Dispersion-less bandpass filters • Arbitrarily sharp • ASE filtering • λ definition in laser cavities	2x2 Optical Switches • Low-loss, all-fiber device • Spatial mode transformation • Exploits modal diversity	Tunable PDL Controllers • Broadband • Enables PMD compensation • Mitigate component PDL	Broadband Amplitude Sensors • Novel sensing mechanism • Simpler diagnostics • Low cost assembly and detection
Tunable Dispersion Control • Wavelength-continuous • Broadband • No tunability/bandwidth tradeoffs. • Use in-line as well as at R_x	Variable optical attenuators • Simple fiber assembly • Potentially very low cost • Use in EDFA control			

the discussions in this paper will focus on the use of long-period fiber gratings (LPGs) as mode converters, but it must be noted that several other device schematics, such as fused fiber couplers and bulk holographic devices exist for providing this functionality, and could be used with few-mode fibers to achieve many of the device functionalities introduced here.

This paper is organized as follows. Section II will introduce the properties of few-mode fiber devices and provide the physical intuition that enables designing them with desired propagation characteristics for various modes. This will be followed by Section III, which will introduce the theory and practice of LPGs, with an emphasis on showing how the device spectra and other characteristics are intimately related to the dispersive properties of the modes of a fiber. These principles will be applied to obtain unique LPG spectra and properties in specially designed few-mode fibers, as will be described in Section IV. Following that, Section V will elucidate demonstrations of novel device applications utilizing the LPGs introduced in Section IV. After discussions on static applications, as mentioned above, the paper will concentrate on tunable devices afforded by the few-mode-fiber design space. Section VI will introduce the theory and practice of novel tuning effects achieved with LPGs written in these fibers, and Section VII will discuss the various device applications that have been afforded by them. Finally, Section VIII will discuss the stability and reliability of LPG devices in few-mode fibers and demonstrate why they are significantly more reliable than conventional LPGs.

II. DISPERSIVE PROPERTIES OF FEW-MODE FIBERS

Fig. 1(a) shows the canonical refractive-index profile of a few-mode fiber, along with the mode profiles of two modes, in this case, the LP_{01} and LP_{02} modes, at various wavelengths. A signature of HOMs is the existence of one or more "sidelobes" of power away from the central core region. Since the wave equations and boundary conditions governing modal properties in optics are analogous to the equations of motion governing the wavefunction of a particle in a box in quantum mechanics, important physical insight can be gained from quantum-mechanical analogies. The canonical refractive-index profile of a few-mode fiber is akin to a potential distribution with three discrete segments—a core and a ring that have an index

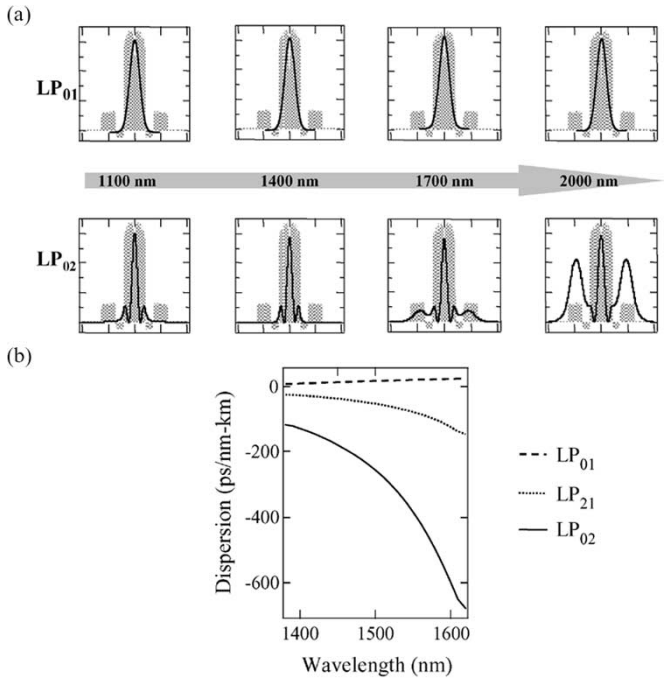

Fig. 1. (a) Mode evolution with wavelength. Grey background is the refractive-index profile. Different modes expand at different rates. Modal expansion is intimately related to propagation properties. (b) Different modes exhibit significantly different dispersive behavior.

greater than silica, which act as attractive wells for light, and a down-doped trench, which acts as a barrier. The indices and thicknesses of these three regions govern the "rate," as a function of wavelength, with which the mode transitions from residing primarily in the core to "escaping" to the ring. Thus, a fiber can be designed with a given refractive-index profile to yield a desired modal rate of expansion as a function of wavelength. Moreover, for paraxial waves, the propagation constant β, of a mode can be expressed in terms of the mode field, as well as the refractive-index profile, as

$$\beta^2(\lambda) \leq \left(\frac{2\pi}{\lambda}\right)^2 \iint n^2(r,\lambda) \cdot |E(r,\lambda)|^2 \cdot \mathrm{d}A \qquad (1)$$

where λ is the free-space wavelength of light, $E(r,\lambda)$ is the mode-field distribution, $n(r,\lambda)$ is the refractive-index profile

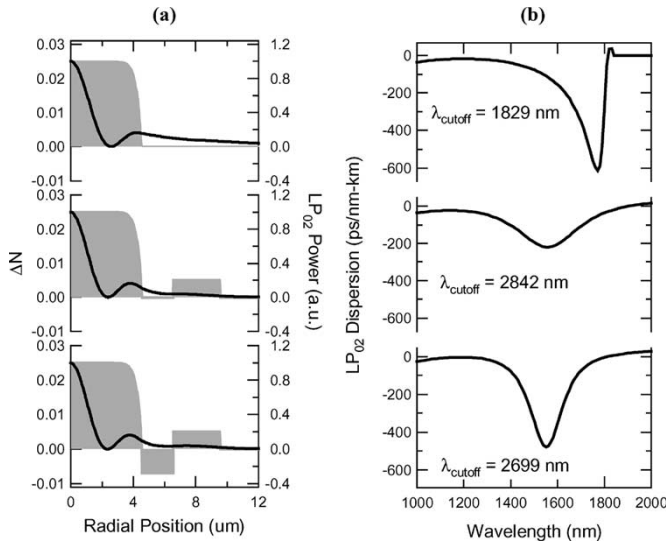

Fig. 2. (a) LP_{02} mode profiles at the most dispersive wavelength (solid lines) in fibers with different refractive-index profiles (gray background). (b) Corresponding plots of LP_{02} dispersion versus wavelength. Profile with a single core: dispersive mode expands into the cladding, has rapidly varying dispersion values, and operates close to cutoff. The addition of a ring yields dispersion far from cutoff, and a trench controls the magnitude of dispersion.

of the fiber, and $\iint \mathrm{d}A$ signifies an integration across the cross-sectional area of the fiber. Equation (1) shows that the propagation constant of a mode is approximately proportional to the average refractive index of the region in which light exists, weighted by the local intensity profile. Combining this concept with the intuition for designing fibers with specific mode profiles at various wavelengths yields the general recipe for tailoring the refractive-index profiles of a fiber to obtain desired values for $\beta(\lambda)$, and all its wavelength-dependent derivates for any spatial mode guided by the fiber. Since $\beta(\lambda)$ and its wavelength-dependent derivatives, such as group velocity, dispersion, etc., are essentially the properties of interest, the intuition elucidated above provides a powerful tool for designing fibers. For example, a mode expanding rapidly with wavelength would have a larger dispersion than a spatially stable mode, and this concept has been exploited to realize low-loss high-figure-of-merit DCFs [8], [9].

HOMs provide greater design flexibility in this respect. Note, from Fig. 1(a), that the rate of expansion is not only different for different modes, it is also different for the various sidelobes. In addition, a significant fraction of the power remains in the central core, indicating that rapidly expanding modes can be constructed with low bend losses. Fig. 1(b) shows the dispersion of various modes in a fiber and shows that the modes of different orders are significantly different in dispersive behavior.

Fig. 2 illustrates a generic design recipe for obtaining desired dispersive properties with an HOM (the LP_{02} mode) by using complex index profiles comprising a central high-index core and adjacent downdoped trenches and rings. The three refractive index and mode-profile plots shown in Fig. 2(a) are for a fiber with only a core (top), a core and a ring (middle), and a complex fiber with a core, ring, and trench (bottom), respectively. The corresponding LP_{02} mode dispersion is shown in Fig. 2(b). The mode profiles represent the mode at its most dispersive wavelength [minima of the curves in Fig. 2(b)]. A fiber with only a core yields very high dispersion values for the HOM, but this occurs close to cutoff—correspondingly, note that the mode profile extends into the cladding. The first demonstration utilizing an HOM (LP_{11} mode) for dispersion compensation used a similar "matched-clad" profile, and while the reported dispersion was as high as -700 ps/nm-km, the fiber also had losses exceeding 1 dB/km [10]. The addition of a ring [middle plots of Fig. 2(a) and (b)] serves two purposes: 1) It confines the LP_{02} mode, yielding substantially longer cutoff wavelengths, and hence, lower losses, and 2) it yields a smoothly varying dispersion curve, which allows the tailoring of the dispersion slope, and is also beneficial from a manufacturing standpoint, because dispersive features do not vary uncontrollably rapidly. Of course, this is evident from the discussion related to Fig. 1, where we note that two attractive regions for light (the high-index core and ring) facilitate controlling the rate of expansion of the sidelobe of the LP_{02} mode, which in turn allows the tailoring of the shape of the dispersion curve [due to (1)]. Finally, the addition of a trench enables the control of the magnitude of dispersion, thus providing simultaneous control over losses, dispersion magnitudes, and dispersion slopes, while providing tolerance to fabrication variations. Such enhanced design flexibility in achieving a variety of desired propagation properties, in conjunction with the fact that light can be shuffled between various modes, makes feasible a variety of novel devices and effects, as will be described in the following sections.

III. Mode Conversion With LPGs—Device Principles

LPGs offer coupling between copropagating modes of a fiber and are attractive as spectral shaping elements and mode-conversion devices. Coupling between two copropagating modes in a fiber occurs when the grating period is adjusted to match their beat frequency. This behavior can be characterized by a phase-matching relationship given by [11]

$$\delta(\lambda) = \frac{1}{2}\left(\Delta\beta(\lambda) - \frac{2\pi}{\Lambda}\right) \tag{2}$$

where δ is a detuning parameter, Λ is the grating period, and $\Delta\beta$ is the difference in propagation constants between the two modes (which is a function of wavelength λ). As a general rule, maximum mode coupling occurs at the resonant wavelength λ_{res}, where the $\delta = 0$ condition (the resonance condition) is satisfied. An intuitive picture of the spectral dependence of LPG couplers can be obtained by considering the phase-matching curve (PMC) of a fiber, which is a plot of the grating period with respect to wavelength at resonance [i.e., a plot of Λ versus λ_{res} when $\delta = 0$, in (2)], shown in Fig. 3(a). Fig. 3(b) shows the corresponding grating spectrum obtained. The coupling magnitude decreases monotonically, at wavelengths away from λ_{res}, that is, as δ departs from 0 in the PMC. Moreover, the bandwidth of the spectrum in Fig. 3(b) is strongly coupled to the gradient of the PMC in Fig. 3(a). The slope of the PMC

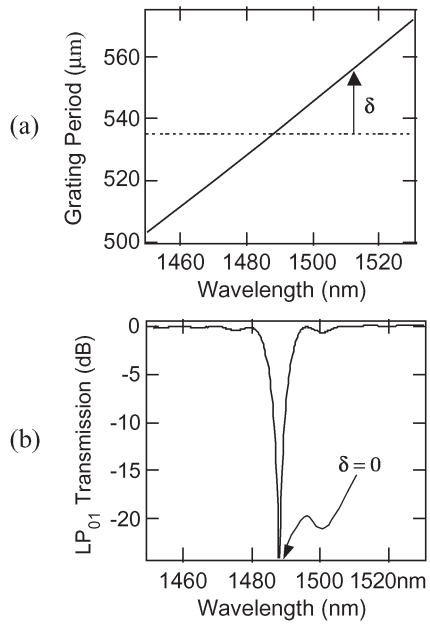

Fig. 3. (a) PMC (plot of Λ versus λ when $\delta = 0$). Dashed line represents grating period. (b) Maximum coupling at $\delta = 0$, decreases as δ departs from 0.

$(\mathrm{d}\Lambda/\mathrm{d}\lambda)$ and the bandwidth of the corresponding spectrum $\Delta\lambda_{\mathrm{bandwidth}}$, respectively, are given by

$$\frac{\mathrm{d}\Lambda}{\mathrm{d}\lambda_{\mathrm{res}}} = -2\pi\frac{\Delta\beta'}{\Delta\beta^2} \tag{3}$$

$$\Delta\lambda_{\mathrm{bandwidth}} \propto \frac{1}{\Delta\beta'} \tag{4}$$

where $\Delta\beta'$ is the slope with respect to wavelength of the difference in the propagation constants between the two modes, and all other terms have been defined earlier. Thus, the bandwidth of the resonance decreases as the quantity $\Delta\beta'$ and, correspondingly, the slope of the PMC increases. The quantity $\Delta\beta'$ is proportional to the difference in group delays $[\Delta\tau_{\mathrm{g}} = -(\lambda^2/2\pi c)\Delta\beta']$ between the two modes, and (3) and (4) can be understood in the following physically intuitive manner. At the resonant wavelength, the phases of the two modes are matched by the grating vector, yielding the condition $\delta = 0$ in (2) and maximal coupling. The strength of the resonance away from this wavelength is governed by the rate of dephasing between the two modes, which is governed by the next higher order Taylor term in the expansion of the propagation constant, namely the group delay.

More generally, the spectral response of an LPG is governed by the spectral evolution of the detuning parameter δ. Since the wavelength-dependent quantities in δ are the propagation constants of modes in a fiber, an LPG spectrum is strongly coupled to the dispersive nature of the fiber itself. Equation (2) may be rewritten as a Taylor expansion about the resonant wavelength λ_{res}:

$$\delta(\lambda) = \frac{1}{2}\left(\Delta\beta'(\lambda_{\mathrm{res}})\cdot\Delta\lambda + \frac{\Delta\beta''(\lambda_{\mathrm{res}})}{2!}\cdot\Delta\lambda^2 + \frac{\Delta\beta'''(\lambda_{\mathrm{res}})}{3!}\cdot\Delta\lambda^3 + \ldots\right) \tag{5}$$

where the primes represent derivatives with respect to wavelength, and $\Delta\lambda$ is the difference between the wavelength of interest and the resonant wavelength. These derivatives are related to physically relevant parameters: $\Delta\beta' \sim \Delta\tau$, the differential group delay, $\Delta\beta'' \sim \Delta D$, the differential dispersion, and $\Delta\beta''' \sim \Delta D'$, the differential dispersion slope, etc. Thus, the spectrum of an LPG may be precisely tailored by adjusting well-known fiber-design parameters, whose control was outlined in Section II.

This provides an additional degree of freedom in the ability to obtain phase matching that is not available in conventional bulk optic-diffraction gratings. LPGs in SMFs have exploited this design space to make sensitive strain and temperature sensors [12], [13], spectrally narrow acoustooptic gratings [14], VOAs [15], and thermally tunable LPGs [16], to name a few devices. While some device-design flexibility is available with the numerous cladding modes in SMF, fully exploiting the intimate connection between fiber-design parameters and LPG spectra is feasible only with few-mode fibers, where both the fundamental mode, as well as the HOM, can be dispersion engineered, as demonstrated in the following sections.

IV. LPGS IN DISPERSION-TAILORED FEW-MODE FIBERS

As illustrated in the previous section, LPG spectral engineering can be achieved by tailoring few-mode fibers with desired dispersive properties. This has especially proven attractive to construct broadband mode-conversion devices, which will be described in detail in this section.

A. Broadband Mode Converters

The concept of broadband mode conversion was first demonstrated by Poole *et al.* [10] in a fiber designed to support the LP_{01} and LP_{11} modes with identical group delays at a predetermined wavelength. Note from (4) that the bandwidth $\Delta\lambda$ of an LPG is inversely proportional to the difference in group delays $(-\Delta\beta')$, and thus, a fiber with identical group delays would be expected to yield very large bandwidths. Periodic microbends, which are used to couple between the fundamental mode and an LP_{11} mode in this fiber, yielded strong mode conversion (> 10 dB) over a bandwidth as large as 74 nm. The few-mode fiber with identical group velocities was designed by operating the HOM (the LP_{11} mode, in this case) close to cutoff.

The operation principle for such fibers is illustrated in Fig. 4, which shows the mode profiles of the fundamental mode, as well as the LP_{02} mode, at two different wavelengths. At a short wavelength $\lambda = \lambda_1$, when the LP_{01} and LP_{02} modes are well guided and reside predominantly in the core of the fiber [Fig. 4(a), left], the ray picture [Fig. 4(b), right] for waveguides accurately predicts that the group delay $[-\beta'(\mathrm{LP}_{02})] > [-\beta'(\mathrm{LP}_{01})]$, since the LP_{02} mode travels at steeper bounce angles compared to the LP_{01} mode. At a longer wavelength $\lambda = \lambda_2$, most of the energy of the LP_{02} mode resides in the low-index ring [Fig. 4(b)], and the mode picture is better suited to gain an intuitive understanding of mode propagation. As the wavelength of operation is increased, the power fraction of the LP_{02} mode in the low-index

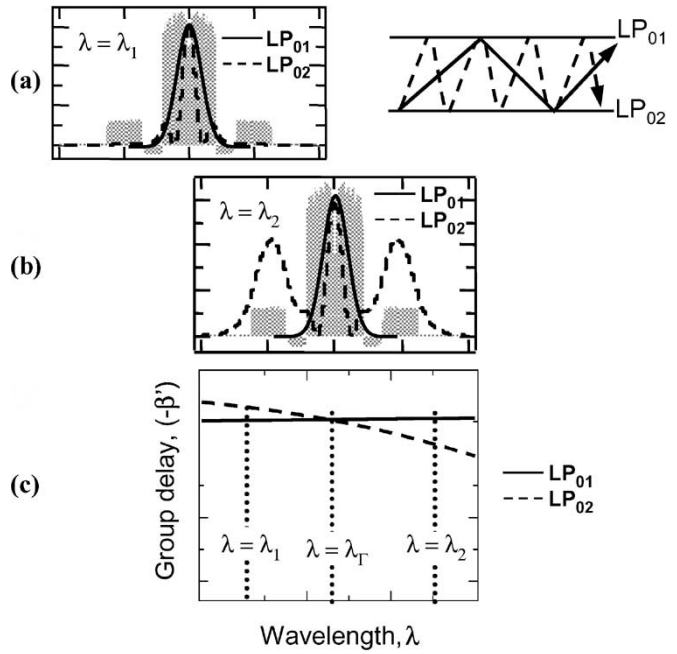

Fig. 4. Dependence of modal delay on mode profile. Grey background is the refractive-index profile. (a) Mode profiles at short $\lambda = \lambda_1$ (left), corresponding ray picture (right). (b) Mode profiles at long $\lambda = \lambda_2$; LP_{02} travels in the lower index regions. (c) Modal delay for LP_{01} and LP_{02}; equal modal delays at intermediate wavelength $\lambda = \lambda_T$.

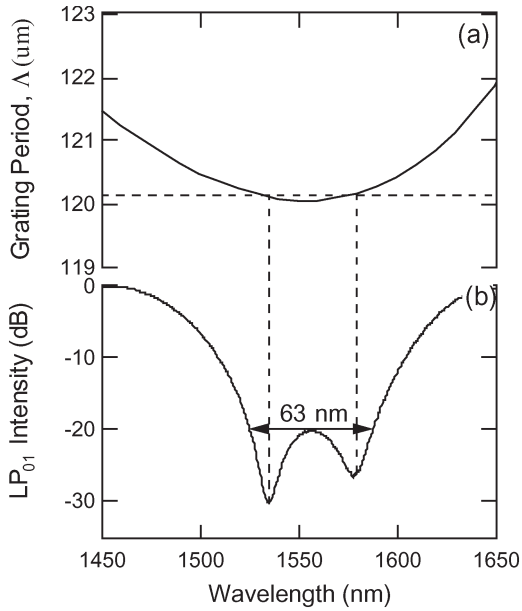

Fig. 5. (a) Simulation: Grating PMC in dispersion-tailored fibers. Large bandwidths obtained at TAP. (b) Experiment: Resultant TAP-LPG spectrum. Peak coupling > 30 dB. More than 20-dB (99%) coupling over 63 nm. Horizontal dashed line indicates the grating period and shows the correspondence between the PMC and the grating spectrum obtained.

ring increases, and its group velocity approaches that of light propagating primarily in the ring (which is higher than that of the core, since it has a lower index of refraction compared to the core). Now, $[-\beta'(\mathrm{LP}_{02})] < [-\beta'(\mathrm{LP}_{01})]$—the LP_{01} mode continues to be well guided, and thus, no significant change is expected for $\beta'(\mathrm{LP}_{01})$. Hence, at an intermediate wavelength $\lambda_1 < \lambda_T < \lambda_2$, the group delays of the two modes match, as shown in Fig. 4(c).

Thus, $\Delta\beta'$ changes sign and this implies that the slope of the phase-matching relationship (3) changes polarity. The result is a turn-around point (TAP) in the PMC, as shown in Fig. 5(a). Following the intuitive rule from Section III, inspection immediately reveals that large bandwidths are attainable if the grating period (shown by the horizontal dashed line) is chosen to couple at the TAP. This is because the dashed line representing the grating period does not depart from the PMC over a large wavelength range. In other words, the resonance condition $\delta = 0$ is satisfied over a larger wavelength range.

Designing fibers that possess a TAP, thus, entails that the HOM rapidly transitions from being guided primarily in the core to one with substantial energy in the lower index ring or cladding (since this ensures that the HOM transitions from the well-guided regime to the "ring" or cladding-guided regime, within the spectral range of interest). Hence, such a fiber should have a core with index and thickness to provide strong guidance to the LP_{01} mode, but weak (almost cutoff) guidance for the HOM, just below the desired TAP wavelength. In addition, the fiber should have a lower index ring in proximity to the core, so that the HOM is confined to it at wavelengths longer than the TAP wavelength, i.e., at wavelengths where a fiber with just the core would not support an HOM. The spectral rate of transition of the HOM is controlled by the indices and widths of the trench and the ring, as in the case of dispersive control of HOM fibers described in Section II. Such dispersive control further enables controlling the curvature of the PMC at TAP, which can be used to control the bandwidth of the TAP resonances, as will be described in Section IV-B. Note that the design recipe does not require that the HOM be close to cutoff but that a fiber that had only a similar core without the trench and ring support an HOM close to cutoff. Fibers yielding TAPs in the PMC between the LP_{01} and LP_{02} modes were fabricated by modified-chemical-vapor deposition (MCVD). The LPGs were fabricated in hydrogen-loaded fibers by a UV laser imaged onto the fiber through an unchirped amplitude mask. The grating period was adjusted to yield a resonance at the TAP.

Fig. 5(b) shows the spectrum of light in the LP_{01} mode, after the LP_{02} mode has been stripped out, for a 1-cm long LPG in a fiber with a TAP at 1540 nm. The grating period for coupling at the TAP of this fiber is 120.2 μm—at this period, the resonance of the PMC is satisfied at two distinct wavelengths because of the existence of a TAP, as shown in Fig. 5(a). The resultant spectrum yields more than 99% mode conversion over a record wavelength range of 63 nm [17] (a 20-dB resonance represents a reduction of LP_{01} power by 20 dB, which, by reciprocity, implies $1 - 10^{-20/10} = 0.99$, or 99% conversion efficiency). In comparison, a 20-dB strong resonance in a conventional LPG typically extends over only ~ 1 nm. The insertion loss of this LPG is < 0.2 dB. In addition, the wavelength range of such a coupling may easily be tuned by scaling the fiber dimensions, thus facilitating a mode converter that works over any wavelength range.

The polarization response of these LPGs is obtained by measuring the variation in output intensity of the LP_{02} mode, with respect to variations in the input polarization state. No

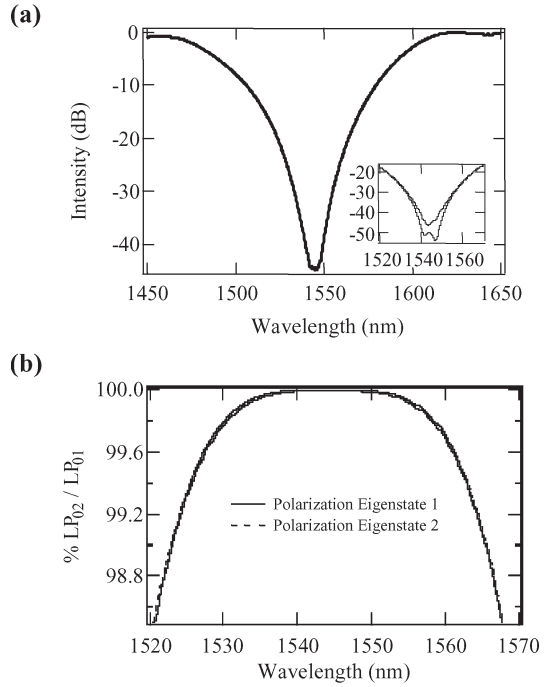

Fig. 6. Polarization dependence of TAP LPG. (a) Spectrum for a strong mode converter; inset shows the polarization-dependent response of the residual fundamental mode. (b) Polarization response of the LP_{02} mode, deduced from data in (a). Spectra barely distinguishable. Peak coupling changes by 0.0002 dB, 20-dB bandwidth changes by 0.2 nm.

measurable change is detected within the measurement accuracy of the external-cavity laser and the photodetector that is used (measurement accuracy $\sim$ 0.02 dB). Significantly higher accuracy can be achieved by measuring the amount of residual fundamental mode in the fiber after the LP_{02} mode is stripped out—for a sufficiently strong LPG, a miniscule amount of the fundamental mode would remain, and small changes in its intensity would result in large variations on a log (decibel) scale. Fig. 6(a) shows the grating spectra for one of the strongest TAP LPGs fabricated—the peak coupling efficiency is $\sim$ 45 dB, with a 40-dB bandwidth of 10 nm and a 20-dB bandwidth of 43 nm. We chose the strongest LPG we have written for this investigation, since it requires the largest UV-induced index change Δn_{UV}, and the polarization dependence of gratings increases with Δn_{UV}. The inset shows the spectra of two orthogonal polarizations corresponding to the largest deviations in grating strength. Fig. 6(b) shows the spectral response of the LP_{02} mode calculated from the data in Fig. 6(a). The spectrum is shown on a linear scale, because small deviations from unity are more visible thus. Even then, the two spectra are barely distinguishable. Variations in input polarization caused the coupling efficiency to range from 99.9960% to 99.9996%, corresponding to a negligible change for applications in optical communications systems. The 20-dB bandwidth also shows a negligible change of $\sim$ 0.2 nm [18]. The polarization-insensitive response of these gratings is expected, since energy for both the modes resides in the core of the fiber. Small perturbations in the circularity of the index profile perturb both modes by similar amounts, and since LPG coupling is sensitive only to the difference in the propagation constants (and not the propagation constants themselves) of the two modes, negligible polarization effects are observed.

It is clear that LPGs in dispersion-tailored fibers possessing a TAP provide an excellent platform for building broadband mode converters. The fiber device is naturally adapted for connecting to a fiber-based transmission line, has very low insertion loss, and practically no polarization dependence. These properties make it very attractive for numerous applications that utilize broadband mode converters, as will be described in Section V.

B. Bandwidth Control of TAP-LPGs

The bandwidth of TAP-LPGs cannot be determined from (4), since the difference in modal group delays $\Delta\beta'$ is zero at the TAP wavelength. Expanding $\Delta\beta$ as a Taylor expansion (5), and retaining the next higher order term (the next higher order term is the modal dispersion $D \sim d^2\beta/\mathrm{d}\lambda^2$), the 20-dB bandwidth of TAP gratings can be obtained as [17]

$$\Delta\lambda \propto \frac{\lambda_{\mathrm{res}}}{\sqrt{\Delta D \cdot L_{\mathrm{g}}}} \tag{6}$$

where ΔD is the difference in dispersion between the two modes, and L_{g} is the length of the grating. As is expected, when the first-order term in the Taylor expansion of β is zero ($\delta\beta' = 0$, identical group delays), the next-order term, differential dispersion $\delta\beta''$, plays a role in determining the bandwidth of the resonance. Just as the gradient of the PMC was related to the difference in group delays $\delta\beta'$, the curvature of the PMC is controlled by the differential dispersion. This is shown in Fig. 7(a), which plots the PMCs for a fiber with a low differential dispersion ΔD at the TAP and one with a high ΔD, respectively. As is evident, the curvature of the PMC at the TAP is lower for the fiber with lower ΔD. Following the insight gained in Section III, it may be inferred that the PMC with lower curvature at the TAP (lower ΔD) will yield a broader LPG bandwidth. This is because the condition $\delta = 0$ is satisfied or nearly satisfied over a larger wavelength range for such a fiber. Indeed, this is also predicted by (6).

This concept is tested by fabricating several fibers with different differential-dispersion values (ΔD) at the TAP. Fig. 7(b) is a comparison of the spectra of TAP-LPG written in fibers with ΔDs of $\sim$ 160, 270, and 520 ps/nm/km, respectively [17]. As expected, fibers with larger differential dispersion show narrower resonances. Note that the values quoted here are the differential-dispersion values (i.e., $\Delta D = D_{01} - D_{02}$) and do not correspond to the dispersion of the LP_{01} or LP_{02} mode alone. In fact, TAP grating bandwidths are independent of the dispersive characteristics of individual modes, and are only a function of the difference in dispersion values between the two modes.

Equation (6) indicates that the bandwidth of TAP gratings is inversely proportional to $\sqrt{\Delta D \cdot L_{\mathrm{g}}}$. Fig. 7(c) shows the experimental and theoretical dependence of the 20-dB grating bandwidth with respect to the parameter $\Delta D^* L_{\mathrm{g}}$. The excellent match between the prediction and the data indicates that (6) accurately describes the behavior of LPG spectra in dispersion-tailored fibers.

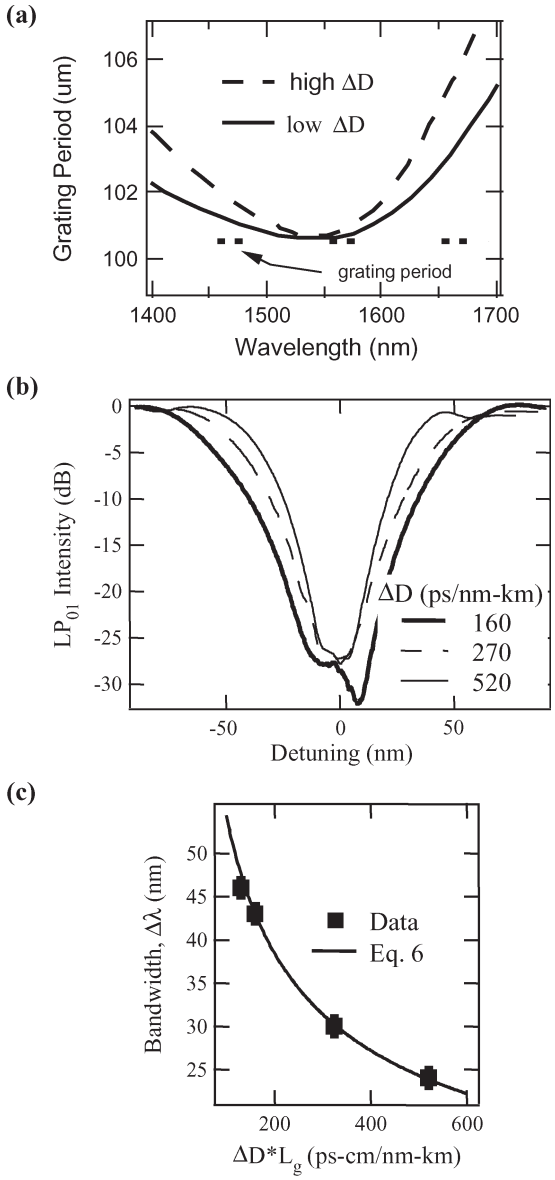

Fig. 7. Control of the LPG spectra by fiber design. (a) PMCs for fibers with low and high ΔD. Higher curvature at TAP for high ΔD fiber. (b) Experimental spectra show that the 20-dB bandwidth increases as ΔD of the fiber decreases. (c) Grating bandwidth versus $\Delta D^* L_{\rm g}$; $L_{\rm g}$ = grating length. Experimental data show an excellent match with the theoretical predictions of (6).

C. Spectrally Flat Coupling for VOA

The previous section illustrated how a fiber can be designed to achieve a variety of grating bandwidths by controlling the differential dispersion. This concept can be extended to unique fiber designs in which several orders in the Taylor expansion of $\delta\beta$, as shown in (5), can be matched. Fig. 8(a)–(c) show the dispersive properties of a few-mode fiber that was designed and fabricated to yield identical group delays, dispersions, and dispersion slopes for the LP_{01} and LP_{11} modes. This implies that several Taylor terms of (5) representing detuning δ are negligible in value. Thus, δ remains close to zero over a large wavelength range, and phase matching is maintained over this enhanced wavelength range.

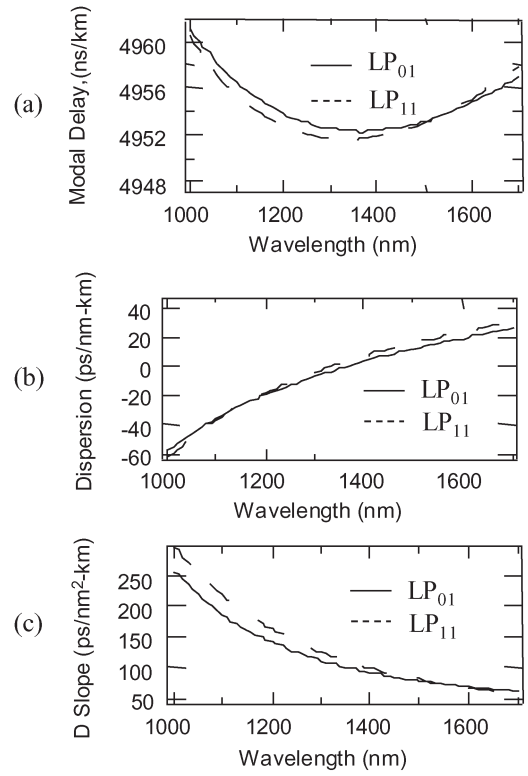

Fig. 8. Taylor terms (5) for LP_{01} and LP_{11} modes. (a) Group delay. (b) Dispersion. (c) Dispersion slope. Close match of curves dramatically enhances the wavelength range of phase matching.

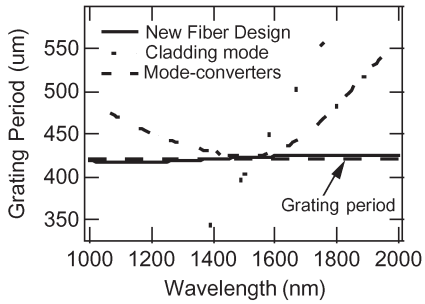

Fig. 9. Grating PMC for various fibers. The PMC of the new few-mode fiber design is almost invariant with wavelength. This implies that phase matching is wavelength insensitive over a large spectral range.

The corresponding PMC for this fiber is shown in Fig. 9. Also shown for comparison, are PMCs for conventional LPGs, as well as the TAP-LPGs described in the previous sections. The PMC is essentially flat throughout a spectral range spanning an octave. As is evident, the line representing the grating period is coincident with the PMC over the whole spectral range. Note that the PMC for this fiber is not strictly horizontal (as designed), but possesses a small amount of curvature, due to small differences in the dispersive properties for the two modes. Nevertheless, the deviation is negligibly small, and gratings coupling the LP_{01} and LP_{11} modes of this fiber would then be expected to be not only broadband but also spectrally insensitive to coupling efficiency.

Microbend-induced gratings were obtained by pressing the fiber between two corrugated aluminum blocks that were machined to yield the desired periodicity of corrugations.

Fig. 10(a) shows the spectrum of a 1-cm long microbend grating induced in this fiber. The 3-dB spectral width is a record value of 565 nm, and since the dispersive parameters are especially well matched in the 1500-nm range, the coupling is also spectrally flat there. The flat spectral region extends over more than 100 nm, as is evident from Fig. 10(a), and the insertion loss, along with the mode strippers, is only 0.2 dB, as is expected of microbend gratings [19].

Attenuation values greater than 10 dB were not achievable in this fiber, because of the inherent polarization sensitivity of microbend gratings. This is because the LP_{11} mode is a superposition of the TE_{01}, TM_{01}, and HE_{21} modes, and each mode has a slightly different PMC [20]. This was confirmed by exciting the grating with polarized light sent through a polarization controller, and observing resonances as deep as 20 dB for specific polarization states, which correspond to the excitation of only one of the three modes existing in the triplet. However, helically induced microbends [21] or microbends on two orthogonal axes [22], as have been proposed to counteract polarization dependence of microbend gratings, may be implemented to yield strong polarization-insensitive VOAs.

Microbend coupling efficiency is a function of the pressure applied by the corrugated blocks on the fiber. This characteristic can be used to construct a cost-effective wavelength-insensitive VOA, as shown in Fig. 10(b), since these gratings exhibit flat spectra over bandwidths as large as 110 nm. Continuous tuning between 0 and 10 dB is achieved with a spectral tilt of less than 0.25 dB over the 110-nm spectral range. Since no fiber-coating removal is required to assemble this device, and more than a million 1-cm long fiber devices can be obtained from a single preform, this device schematic provides for a compact, low-loss, broadband, and potentially cost-effective VOA.

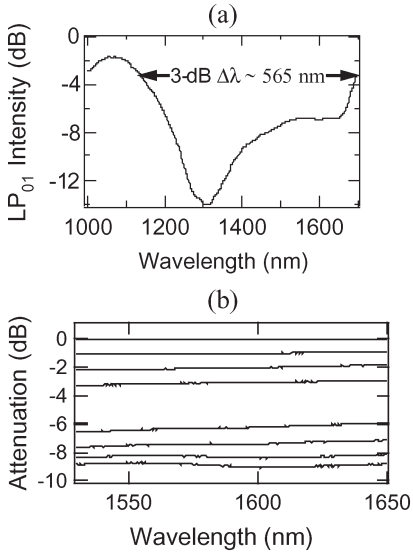

Fig. 10. Microbend grating spectrum in novel few-mode fiber. (a) Grating length = 1 cm. Record 3-dB bandwidth (565 nm) due to the flat PMC shown in Fig. 9. Spectrally flat coupling in the 1550-nm region, where the dispersion parameters of fiber are identical (see Fig. 8). (b) VOA operation in a flat spectral region. Continuous tuning from 0–10 dB in $C + L$-band, with $<$ 0.25-dB spectral tilt.

V. Static Devices Using TAP-LPGS

Section IV introduced a variety of spectral shaping tools accessible by designing dispersion-engineered fibers. One of the most important devices to arise from these concepts is the broadband mode converter using TAP-LPGs. This section will illustrate the device applications it has impacted.

A. Higher Order Mode Dispersion-Compensating Modules (HOM-DCM)

Long-distance high-speed transmission over broad bandwidths requires the careful management of dispersion and nonlinear distortions of the transmitted optical signal. Dispersion, being a linear distortion, can be compensated with a DCM that provides equal dispersion of the opposite sign. Systems requirements dictate that the DCM of choice must be able to compensate for the variety of dispersion slopes of the transmission fibers used in optical links, while being low loss and resistant to nonlinear distortions.

The DCMs widely deployed today are single-mode DCFs, which are relatively low loss and can offer dispersion-slope compensation for a wide variety of transmission fibers [23]. However, single-mode DCF solutions result in propagation through small effective-area fiber ($A_{\text{eff}} \sim 15{-}20\ \mu\text{m}^2$), which causes nonlinear distortions in the signal. Moreover, this technology is also not amenable for providing tunable dispersion in a practical schematic.

An alternative approach is to compensate for dispersion using HOMs. Poole *et al.* first demonstrated this concept by using the highly dispersive properties of the LP_{11} mode to realize DCMs with fiber dispersions as high as -700 ps/nm/km [10]. While that demonstration provided a proof-of-concept for using HOMs for dispersion compensation, there were several drawbacks associated with using the antisymmetric LP_{11} mode that made it not viable for practical applications. As mentioned in Section IV-C, the LP_{11} mode is inherently polarization insensitive, and while it was pointed out that helical gratings may be used to circumvent the PDL problem, the polarization degeneracy also leads to polarization mode dispersion [24], which is hard, if not impossible to combat in a practical device schematic [25]. In addition, dispersive behavior of the LP_{11} mode occurs close to its cutoff [26], yielding very high propagation losses and potentially unstable behavior (with respect to fiber fabrication).

Thus, HOM dispersion compensation with the polarization insensitive LP_{02} mode has received a lot of attention in the recent past, primarily due to its ability to offer dispersion-slope matching to any transmission fiber currently deployed [27], [28] [Fig. 11(a)]. As mentioned in Section II, the dispersive nature of the LP_{02} mode results from transitions in the side lobes of their mode profile with respect to wavelength, while maintaining significant energy in the central core. Thus, they can be expected to yield low loss and high dispersion, without the need to operate close to cutoff. HOM fibers with propagation losses of only 0.44 dB/km and dispersion as high as -210 ps/nm/km have been fabricated, yielding record figures of merit (FOM = dispersion loss $\sim$ 477 ps/nm/dB) [29]. In addition, the effective area of an HOM is approximately

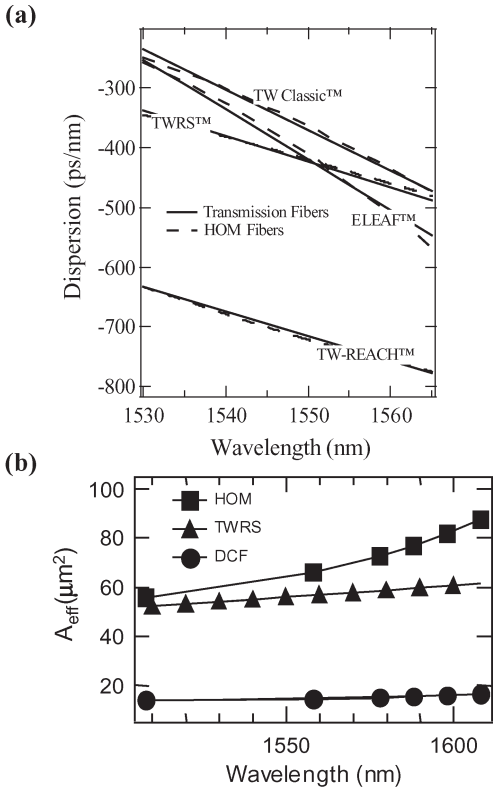

Fig. 11. HOM fibers for dispersion compensation. (a) Solid lines: dispersion-compensation requirement for a 100-km link with different transmission fibers; dashed line: corresponding HOM fiber characteristics. Variety of dispersion and dispersion slopes achievable with LP_{02}—match the dispersion slope of every transmission-fiber type. (b) Effective area of HOM $\sim 4-5 \times$ DCF $\Rightarrow$ lower nonlinearities.

four to five times larger than the fundamental mode in DCFs [Fig. 11(b)], which decreases the impact of nonlinearities.

The schematic of the HOM-DCM is shown in Fig. 12. The device consists of a spool of HOM fiber spliced on to two TAP-LPG-based mode converters that convert the LP_{01} mode into the LP_{02} mode and vice versa at the input and output of the module, respectively. Since the HOM fiber intrinsically supports more than one propagating mode, an important consideration while building an HOM-DCM is managing modal-interference noise arising from the beating of light propagating in different modes. Such multipath interference (MPI) is characterized by the ratio of signal power that may have traveled in spurious modes to that in the desired (LP_{02}) mode. Systems tests have revealed that an MPI < -40 dB is needed to ensure that more than 30–40 such compensators can be concatenated in a transmission line, as would be required in long-haul communications links with a DCM in each amplifier hut [30], [31]. This requires that 1) the propagation constants β of different modes in the fiber are substantially separated to avoid in-fiber mode coupling; 2) connections between the mode converter and the HOM fiber (see Fig. 12) are essentially adiabatic in that the LP_{02} mode of the mode-converter fiber does not scatter into the other modes of the HOM fiber; and most importantly, 3) the mode converter offers high mode-conversion efficiency to the LP_{02} mode and high extinction for the other modes.

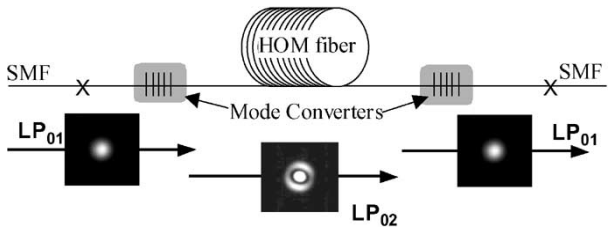

Fig. 12. HOM-DCM schematic. HOM fiber with input and output $LP_{01}-LP_{02}$ TAP-LPG mode converters.

TAP-LPGs, described in Section IV-A, are ideal choices for this mode-conversion operation. They are realized in HOM fibers similar to the dispersive HOM fiber, hence reducing the prospect of spurious coupling to other modes at the splices (measured MPI values for optimized splices have been roughly -50 dB/splice). They are inherently low loss, on account of being an in-fiber device (loss < 0.2 dB—see Section IV-A). Most crucially, they offer strong broadband-mode conversion. Note that all the discussion on bandwidth of TAP LPGs in Sections IV-A and B focused on the 20-dB bandwidth of the gratings. This is because two 20-dB strong gratings concatenated in series (as in the schematic of the HOM-DCM shown in Fig. 12) yield 40-dB modal extinction, which is the minimum desired MPI level required for penalty-free systems operation of HOM-DCMs. Since Section IV-A describes TAP-LPGs with up to 63 nm of 20-dB bandwidths, such gratings can facilitate HOM-DCMs with MPI < -40 dB for bandwidths up to 63 nm. Also note that Section IV-B presented the design recipe to further extend the bandwidths of TAP-LPGs. Hence, HOM-DCMs enabled by TAP-LPGs can potentially have low MPI behavior over bandwidths exceeding currently reported values of 63 nm.

The significant advantage of HOM-DCMs over DCFs is that the signal propagates in a very large effective area—note from Fig. 11(b) that the A_{eff} of HOMs is roughly four to five times that of DCF. This results in higher resistance to nonlinear distortions [32]. This has been confirmed by transmission experiments with (high speed) 40-Gb/s return-to-zero (RZ) signals. Links amplified by EDFAs could transmit signals over 12×100 km of TrueWave reduced-slope (TWRS) fiber when the HOM-DCM was used and 8×100 km when the single-mode DCF was used [Fig. 13(a)] [33]. The 50% increase in transmission distance is attributed to the ability to increase input power into the HOM-DCMs by 10 dB. For hybrid Raman/erbium-amplified systems, 40-Gb/s transmission distances of 1700 km have been enabled by HOM-DCMs, because the OSNR was improved by 1 dB, in comparison to an identical link compensated with DCF [Fig. 13(b)] [34].

The transmission-distance improvements were primarily enabled by the large effective area for the LP_{02} mode and the use of low-loss polarization-insensitive mode converters fabricated with TAP-LPGs.

B. Dispersionless Bandpass Filtering

Broad bandwidth mode converters described in Section IV-A can also be used as spatial mode transformers to realize band-selection filters [35], which have numerous applications,

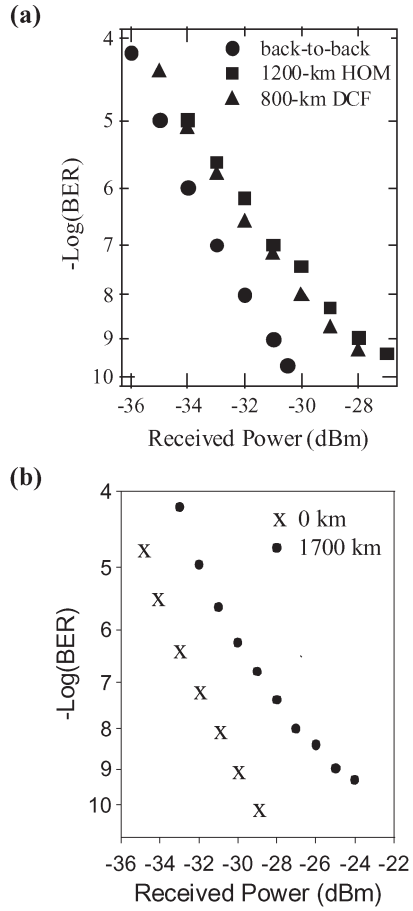

Fig. 13. Transmission experiments with the 40-Gb/s RZ signals. 100-km TWRS + HOM-DCM or DCF. (a) Erbium amplified system—50% transmission-distance increase with HOM. (b) Hybrid erbium/Raman system—1-dB OSNR improvement, enabling 1700-km transmission.

such as frequency selectors for fiber–laser cavities, and amplified spontaneous-emission noise filters in optically preamplified receivers.

The device requires two LPGs that are fabricated in identical fibers that are dimensionally scaled by different amounts—that is, the fiber is drawn from the same preform to different outer diameters (OD). When a few-mode fiber is dimensionally scaled, the phase-matching relationship shifts, such that the TAP now occurs at a different wavelength and grating period, as noted in Section IV-A. This is illustrated in Fig. 14, which shows the PMC for fibers drawn to ODs ranging from 110 to 121 μm. Fig. 14 shows that while an LPG written to couple at the TAP of a few-mode fiber will yield a broadband mode converter, an identical LPG written in the same fiber drawn to a different OD will yield a narrowband resonance expected of conventional LPGs.

The schematic of the bandpass filter is shown in Fig. 15(a), which illustrates that LPGs in few-mode fibers drawn to two different ODs (denoted **I** and **II**) are spliced together to realize the bandpass filter. The spectra obtained by writing LPGs in these two fibers are shown in Fig. 15(b). The PMC for fiber **I** (OD = 121 μm) that has a TAP at 1540 nm [Fig. 15(a)] and an LPG written at the corresponding grating period ($\Lambda =$ 112.5 μm) converts the incoming LP_{01} mode into the LP_{02}

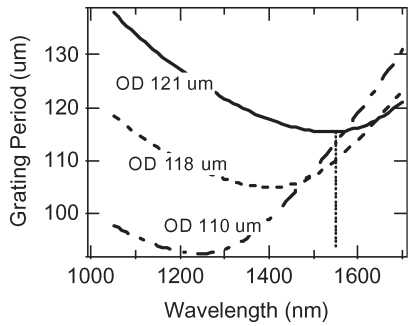

Fig. 14. PMC for LPG in few-mode fibers of different ODs. TAP shifted by dimensionally scaling the HOM fiber.

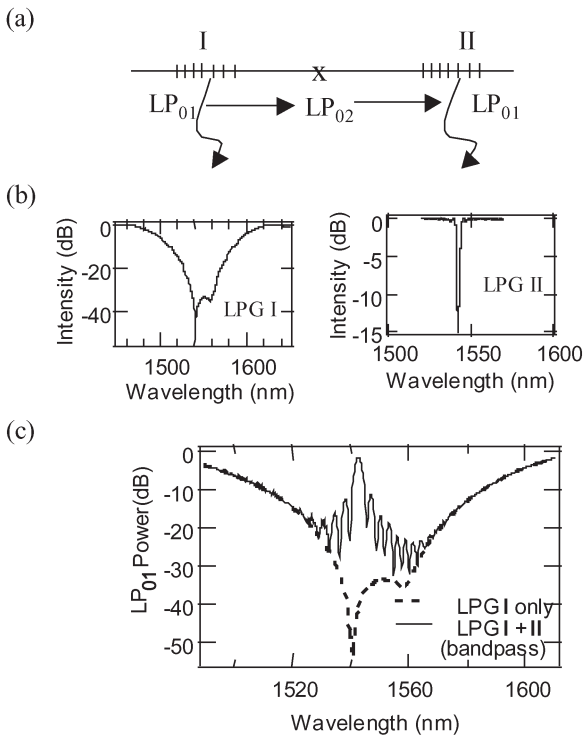

Fig. 15. (a) Bandpass filter schematic—LPG in fiber **I** and **II** spliced. Splice ensures adiabatic transition of LP_{02} mode from fiber **I** to **II**. Arrows show dominant mode of propagation. (b) LP_{01} transmission spectra of LPG **I** and **II**. LPG **I**—broadband TAP resonance, LPG **II**—conventional narrowband resonance. (c) Resultant bandpass spectrum—spectrum defined by the characteristics of LPG **II** alone.

mode over the entire C-band [Fig. 15(b)—left]. Fiber **II** is a similar few-mode fiber, but is drawn to an OD of 112 μm. In the 1550-nm spectral range, the PMC for this fiber exhibits a monotonic variation, as in conventional LPGs. Fig. 15(b) (right) shows the spectrum of a 10-cm long uniform LPG written in Fiber **II**.

All the light in an entire communications band passing through LPG **I** is converted to the LP_{02} mode. Splicing the two fibers converts the LP_{02} mode of fiber **I** adiabatically into the LP_{02} mode of fiber **II**. Then, LPG **II** selects a desired narrow portion of the spectrum back into the LP_{01} mode. This results in a bandpass filter, as shown in Fig. 15(c). The 3-dB bandwidth of this filter is $\sim$ 2.5 nm, and the peak isolation is as high as -35 dB.

Spectral filters are typically dispersive close to their band edges. For instance, the complex amplitude response of a uniform LPG, as deduced from coupled-mode theory is

$$E_{\text{in}} = \left\{\cos^2\left(L\sqrt{\kappa^2+\delta^2}\right) + \frac{\delta^2}{\kappa^2+\delta^2}\sin^2\left(L\sqrt{\kappa^2+\delta^2}\right)\right\}^{\frac{1}{2}} \times \exp\left[i\tan^{-1}\left\{\frac{\delta}{\sqrt{\kappa^2+\delta^2}}\tan\left(L\sqrt{\kappa^2+\delta^2}\right)\right\}\right]$$

$$E_{\text{out}} = \left\{\frac{\kappa}{\sqrt{\kappa^2+\delta^2}}\sin\left(L\sqrt{\kappa^2+\delta^2}\right)\right\}\cdot\exp[i\pi] \quad (7)$$

where E_{in} is the electric-field amplitude of the mode that contains all the power at the input of the LPG, E_{out} is the amplitude of the mode that light is scattered into (which had zero power at the input of the grating), κ is the coupling coefficient, and δ is the detuning. This reveals that while the phase response of E_{out} is not a function of wavelength, the phase response of E_{in} is strongly coupled with its magnitude response. As an LPG becomes spectrally sharp or narrow, the magnitude of E_{in} varies rapidly with wavelength—likewise, the phase response also shows strong wavelength dependence. Thus, it is expected that a signal that passes through a sharp LPG-based band-rejection filter will suffer from dispersion-related penalties. On the other hand, the scattered mode E_{out} has no spectral phase variation and would always be dispersion free.

Since the TAP-LPG-based bandpass filters transmit only the "cross" arm (E_{out}) from LPG **II**, they are expected to be inherently dispersion free. Fig. 16(a) shows the spectra of the gratings in the conventional notch filter and bandpass configuration, respectively. Fig. 16(b) shows their corresponding group-delay (GD) response. For the notch filter, the GD rises sharply with wavelength, resulting in dispersion values as high as ± 10 ps/nm close to the resonance. When the same grating is deployed in the bandpass configuration, the GD remains constant throughout the resonance, implying that these bandpass filters are dispersion free.

Finally, tuning these bandpass filters simply entails tuning LPG **II**, and thus, is amenable to all existing tuning mechanisms for conventional LPGs. Fig. 17 illustrates the temperature-tuning capability of these bandpass filters. Increasing the temperature of the package housing LPG **II** over a range of 180 °C monotonically moves the bandpass resonance from 1538 to 1564 nm. The insertion loss of the filter is only 0.4 dB. The loss varies by approximately 0.2 dB as the filter is tuned over 26 nm.

The loss value of this device ($\sim$ 0.5 dB) is a significant improvement over that of conventional LPG-based bandpass filters, which utilize two identical cladding-mode-coupled LPGs separated by an inline core-mode loss element [36]. Conventional LPG bandpass filters have a 1.5–2 dB loss, primarily because the inline loss element is necessary to attenuate unwanted LP_{01} light that would cause modal interference. This loss element also attenuates a large amount of the coupled cladding mode, because cladding modes have substantial

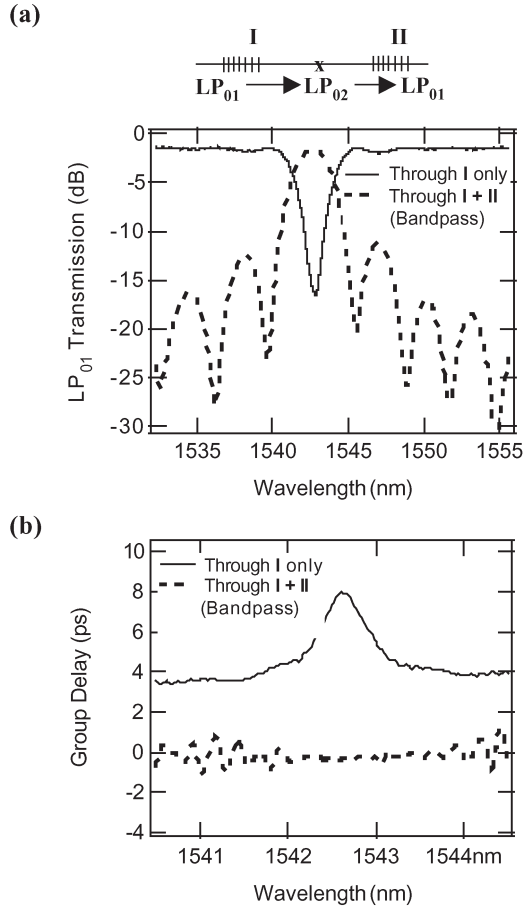

Fig. 16. (a) Transmission and (b) group-delay response for conventional and bandpass filters. The conventional filter is represented as a solid line and the bandpass filter is shown as a dashed line. A 3-dB $\Delta\lambda$ is applied to both (2.5 nm). Conventional filter: $D \sim \pm 10$ ps/nm; bandpass filter is dispersion free.

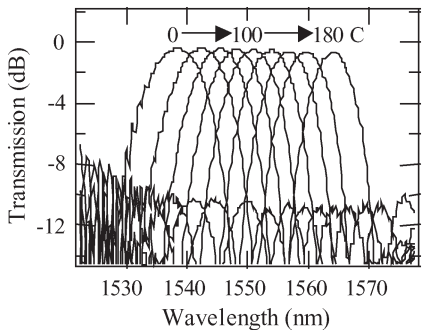

Fig. 17. Tunability and loss characteristics of bandpass LPG. Tuning requires the tuning of LPG **II** only. Thermal tuning of filter—26-nm range with 180 °C temperature change. Filter insertion loss is $\sim$ 0.4 dB.

energy in the core of a fiber. On the other hand, the HOM bandpass filters described here require no extraneous loss elements, because LPG **I** (the TAP LPG) offers broadband mode conversion over a bandwidth that is an order of magnitude larger than the spectrally selective LPG **II**. The only extraneous loss contribution of this device arises from the possibility of a nonadiabatic splice between the two fibers [see Fig. 15(a)]. Since the two fibers are scaled versions of each other, optimizing a splice yields adiabatic transmission of light in the LP_{02} mode through the splice.

The device illustrated in Fig. 15 provides a general platform for building band selection as opposed to band-rejection filters with LPGs. The first mode converter (LPG **I**) only serves as a device that provides a spatially modified input of light for LPG **II** and does not define the spectral characteristics of the bandpass filter. The spectrum of the filter is uniquely defined by the inverted spectrum of LPG **II** alone. This enables the prospect of spectral shaping in the bandpass configuration by varying the spectral properties of LPG **II**. In addition, this device schematic provides the means to make very narrowband, as well as tunable, wavelength selectors that are dispersion free, regardless of bandwidth.

VI. Tunable LPGs in HOM Fibers

Tuning mechanisms for conventional LPGs comprise of either changing the grating period by strain, or shifting the PMC by some mechanism that alters the dispersive properties of one or both the modes that are coupled through the grating. These mechanisms include the thermooptic effect (induced by temperature-induced changes of the waveguide properties), stress-optic effect (pressure-induced refractive-index changes), electrooptic effect, or any other effect that essentially changes the refractive-index profile of the fiber. This leads to changes in the propagation constants of one or both modes, as is evident from (1), which in turn shifts the PMC [as is clear from (2)]. Correspondingly, the wavelength at which the line representing the grating period intersects the PMC shifts (see Fig. 3), moving the entire LPG spectrum to be centered at the shifted resonant wavelength. Strain directly changes the grating period [and thus, the position of the grating line in Fig. 3(a)] to shift the resonant wavelength. In either case, the tuning mechanism does not dramatically change the gradient of the PMC, and thus, tuning results in the reproduction of an identical spectrum at a new resonant wavelength. Such tuning effects have resulted in a variety of tunable devices comprising conventional LPGs, and have also been applied for tuning the dispersion-free filters described in Section V-B. On the other hand, tuning TAP-LPGs results in amplitude changes in the spectrum rather than wavelength shifts, due to characteristics unique to their PMCs. This novel effect will be described in this section, and will be applied to novel device functionalities in the following sections.

A. Amplitude Modulation: Novel Detuning Effects in TAP-LPGs

Fig. 18(a) shows the now-familiar PMC of TAP-LPGs, along with three horizontal dashed lines representing grating periods Λ_{T}, Λ_{A}, and Λ_{B}, where Λ_{T} corresponds to grating-coupling at the TAP, and the two other grating periods lie in regions where they do not intersect the PMC at any wavelength. The phase-matching condition of (2) may be recast in terms of this PMC as

$$\delta = \pi \left(\frac{1}{\Lambda_{\mathrm{TAP}}(\lambda)} - \frac{1}{\Lambda} \right) \tag{8}$$

where Λ_{TAP} is the grating period required for resonance along the PMC [i.e., the plot of the curve shown in Fig. 18(a)], and Λ is the actual LPG period, taking values Λ_{T}, Λ_{A}, and Λ_{B}, shown in Fig. 18(a). The corresponding spectra obtained at these periods are shown in Fig. 18(b). For $\Lambda = \Lambda_{\mathrm{T}}$, coupling occurs at the TAP, and the familiar broadband resonance, described in Sections IV-A and IV-B, is obtained. However, for a grating with $\Lambda = \Lambda_{\mathrm{A}}$ and $\Lambda = \Lambda_{\mathrm{B}}$, no resonance occurs because the grating period does not intersect the PMC at any wavelength. In terms of (8), this represents a condition where $\delta \neq 0$ for any wavelength. In this case, the spectrum somewhat resembles that of a TAP resonance, but with diminished coupling strength. Moreover, the coupling efficiency for the grating with $\Lambda = \Lambda_{\mathrm{B}}$ is weaker than that for the grating with $\Lambda = \Lambda_{\mathrm{A}}$, since δ is larger in magnitude throughout the spectral range. Thus, the coupling efficiency for TAP-LPGs decreases roughly monotonically, as the grating period departs from the TAP grating period Λ_{T}, while maintaining its spectral shape. This is in significant contrast to conventional LPGs, where changing the grating period would merely shift the resonance in wavelength.

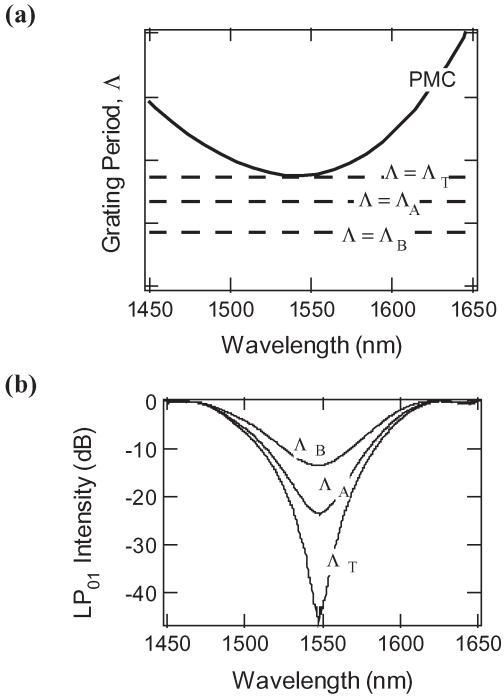

Fig. 18. Novel detuning effects in TAP-LPGs. (a) Typical PMC for few mode-fibers. Horizontal dashed lines represent grating periods at and away from TAP. (b) Resultant spectra. Coupling efficiency decreases as the grating period departs from the TAP-period Λ_{T}. There is no phase matching at any λ for grating periods Λ_{A} and Λ_{B}. Hence, a diminished resonance with the same shape results.

This offers a powerful new tuning mechanism that can be applied to assembling cost-effective temperature, strain, or ambient index sensors. Changes in the control parameter (strain, temperature, etc.) would serve to change the throughput transmission of the LPG, leading to a sensing system that comprises a cost-effective broadband LED connected to a power detector though a TAP-LPG. Fig. 19(a) and (b) show the spectral changes to a TAP-LPG in response to temperature and strain changes, respectively. Note that the sensitivity obtained by this mechanism (a 1-dB change in transmission for a 4 °C temperature shift or 0.002% strain, for a 1-cm long TAP-LPG) is significantly higher than that for conventional LPG

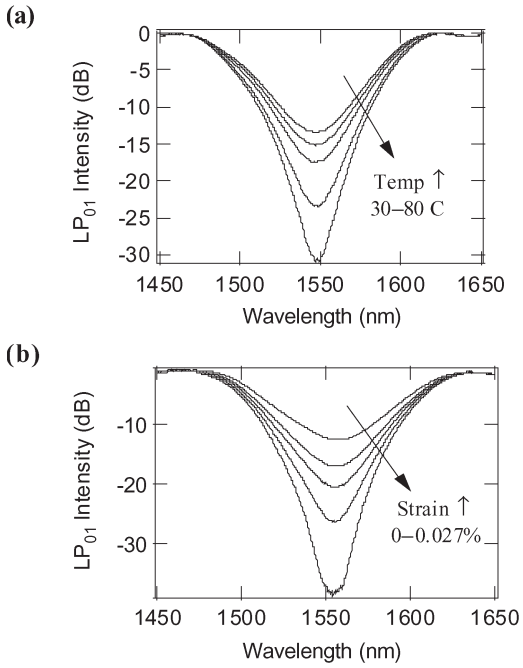

Fig. 19. TAP-LPGs as sensitive (a) temperature and (b) strain sensors. 1-cm long LPG: 1-dB change in transmission for 4 °C temperature shift or 0.002% strain.

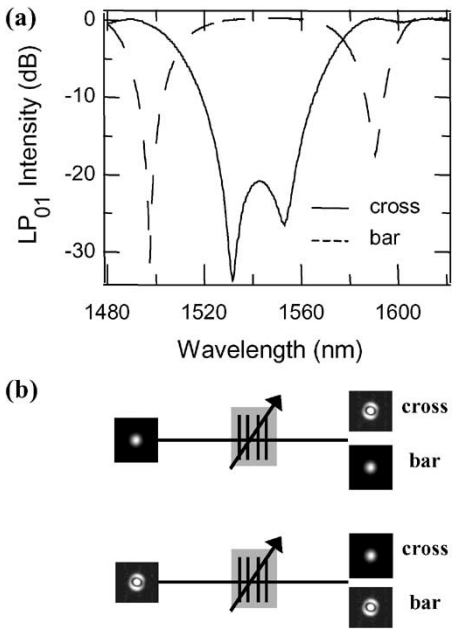

Fig. 20. 2×2 switches with TAP-LPGs. (a) Spectrum of switch showing strong (cross state) or no (bar state) mode conversion. (b) Near-field images of the modal input and output at the cross and bar states.

sensors, since small changes in power levels can be measured much more accurately than small wavelength shifts. Moreover, the sensitivity will increase linearly with the length of the grating, and since the bandwidth and the length of the grating can be decoupled by designing a fiber with desired dispersive properties, arbitrarily high sensitivities can be achieved.

B. Switching and Routing

The novel amplitude-tuning mechanism demonstrated in the previous section can be applied for assembling two-state switches instead of continuous modulators. Toggling the LPG between a state that represents coupling at the TAP, and another that yields identically zero coupling over a broad bandwidth, yields 2×2 switches, as shown in Fig. 20. Fig. 20(a) shows the spectrum of the switch in the cross and bar states, respectively. Since LPGs are reciprocal devices, input light in either mode can be switched to an output, again in either mode, simply by switching the LPG between the cross and bar states, as the experimentally measured mode profiles in Fig. 20(b) show. The switching action was induced by packaging the LPG in a stainless-steel package, which when heated, applies a strain, as well as a temperature shift, in the PMC. Thus, only moderate temperatures are required for the switching action—switching these LPGs from the cross to the bar states involved changing the temperature on the packages between 50 and 120 °C.

VII. Tunable TAP-LPG Devices

Section VI introduced some novel tuning capabilities of TAP-LPGs, which allows for both continuous operation, as well as discrete switching. In analogy with the static devices, the tunable LPGs offer a low-loss means to achieve device functionality, and the use of few-mode fibers enables dispersion tailoring of the spectral responses. This section will describe examples of devices that exploit the continuous tuning capability, as well as the discrete switching functionality of TAP-LPGs.

A. Tunable/Adjustable HOM-DCMs

As mentioned in Section V-A, dispersion management is a critical requirement in optical-communications links. Statistical variations in the dispersion of transmission fibers, amplifier-hut spacings, or ambient conditions can lead to significant transmission penalties, because of variations in accumulated dispersion. One way to address this problem is by introducing TDCs, which can provide either a dynamic control or a control that can be set. Most TDCs demonstrated to date rely on the phase response of optical filters, which have bandwidth versus tunability tradeoffs and operate only within well-defined periodic passbands.

Since few-mode fibers guide more than one mode with different group delays and dispersion, the inherent optical-path diversity is naturally suited to realize TDCs that can provide control that can be set. Fig. 21(a) shows the device schematic for an HOM device, which comprises five segments of HOM fibers, arranged in a binary length progression, with switchable TAP-LPGs (see Section VI-B) between each segment. Since this HOM fiber supports the LP_{01} and LP_{02} modes, two optical paths exist in each segment, leading to $2^5 = 32$ distinct optical paths (and thus, 32 distinct dispersion values). Fig. 21(b) shows the dispersion-tuning capability of this device [37]—a tuning range of 435 ps/nm is achieved over a 30-nm bandwidth, with an average insertion loss of only 3.7 dB, which is lower than that of colorless TDCs constructed with any other technology.

To test the performance of these TDCs, carrier-suppressed RZ signals were transmitted through a span comprising TWRS and TW-Reach fibers (span dispersion $\sim +377$ ps/nm at 1545 nm). The device switch state was adjusted to yield

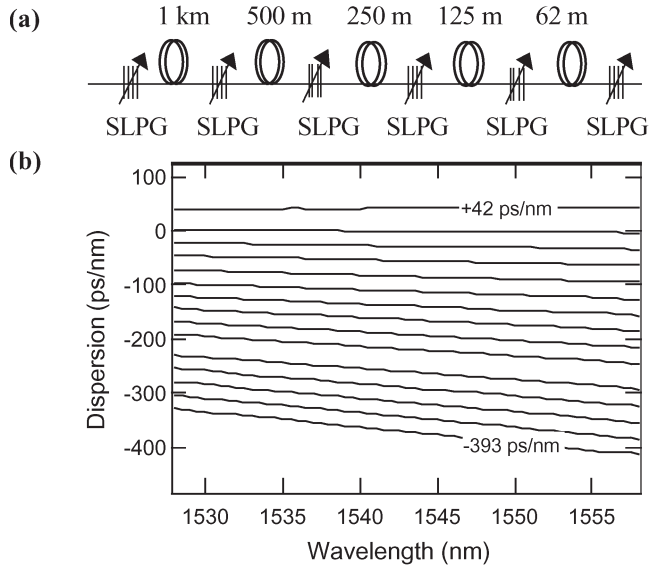

Fig. 21. (a) Adjustable HOM schematic—binary-length progression of HOM fibers with switchable LPGs as 2×2 switches. (b) Dispersion versus wavelength. Tuning range $= 435$ ps/nm, wavelength-continuous response over 30 nm.

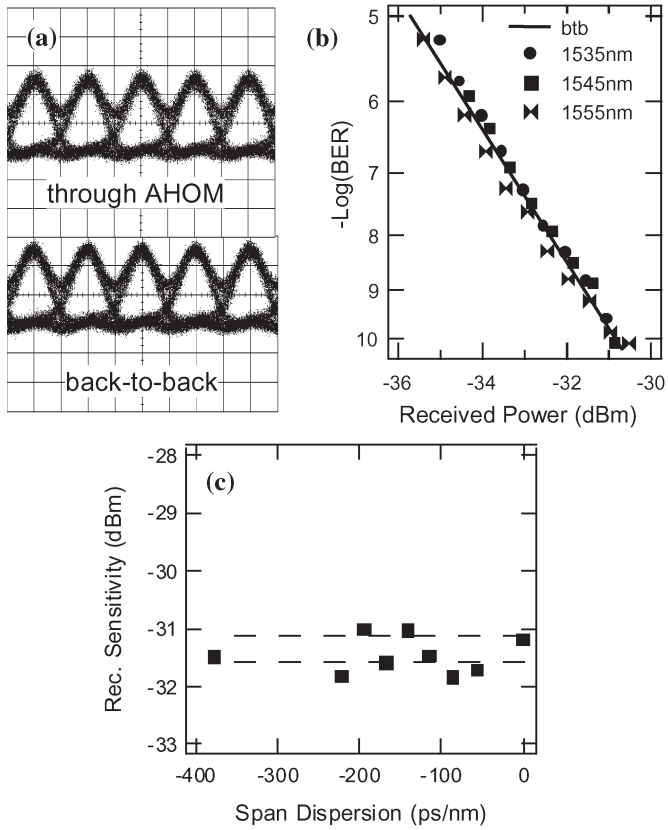

Fig. 22. (a) Forty-Gb/s eye diagrams for a span with dispersion $= 377$ ps/nm and TDC at -378 ps/nm at 1545 nm. (b) BER curves for 40-Gb/s carrier-suppressed RZ—penalty-free operation at wavelengths across the C-band. (c) Received power for BER $= 10^{-9}$, for different fiber spans + TDC states. Penalty-free operation over entire tuning range.

-378 ps/nm at 1545 nm. The open eye in Fig. 22(a) qualitatively confirms the distortion-free dispersion-compensating capability of the device. To quantify this, BER measurements were conducted for the same span at 1535, 1545, and 1555 nm, respectively. Fig. 22(b) shows that the BER curves at all three wavelengths essentially overlap with the back-to-back measurement, indicating that the device is broadband, and offers penalty-free performance.

The dispersion-tuning characteristic of the device was tested by measuring receiver sensitivities at a BER of 10^{-9} for 40-Gb/s 1545-nm signals. Several different transmission-fiber spans (comprising combinations of TWRS and TW-Reach fibers) with different lengths were assembled, and the adjustable HOM-DCM was tuned to the appropriate values to yield the closest match in dispersion. Fig. 22(c) shows the receiver sensitivity for the different spans (with different dispersion values) compensated by the TDC tuned to the corresponding optimal state. The two horizontal dashed lines show back-to-back receiver sensitivities from two separate measurements, indicating 0.4-dB measurement uncertainty. As is evident from Fig. 22(c), penalty-free transmission (within the measurement error) is achieved for switch states spanning the entire tuning range of the TDC.

The significant distinction from other TDCs is that this device is simultaneously broadband and wavelength continuous. Thus, it may be deployed inline, as well as at the receiver, and is not constrained to operation at specific bit rates, bit formats, or channel spacings. Furthermore, there are no inherent tradeoffs between tuning range and bandwidth, as is the case for other TDCs.

B. Polarizers and PDL Controllers

PDL, which induces random fluctuations in the OSNR of an optical link, can severely degrade systems performance. In-line polarizers and PDL compensation may offer a means of addressing this problem. This section describes the use of HOM fibers and TAP-LPGs to construct such devices.

In Section V-B, the discussion about TAP-LPG-based bandpass filters had introduced the concept of dimensional scaling to shift the PMC and TAP of the HOM fiber. Similarly, if form birefringence is introduced in the fibers, it can be expected that two distinct PMCs and TAPs would exist for orthogonally polarized light entering the LPG. Fig. 23(a) shows the PMCs for an HOM fiber fabricated with 2% ovality in the cross-sectional dimensions of its core. The figure shows that 1) two PMCs are obtained—one for each orthogonal state of polarization (SOP) for light in the fiber and 2) both curves show a TAP.

Writing an LPG in this fiber yields a polarizer, whose polarizability can be adjusted by varying the index change during fabrication. Fig. 23(b) shows the spectra of 20-dB-strong 5-cm-long gratings written in these fibers, with a grating period of 90.25 μm, corresponding to the dashed line in Fig. 23(a). The plots show the grating spectra for the two orthogonal SOPs, $+$ and $\|$. SOP $\|$ yields a broadband spectrum, since the grating period is at the TAP for this polarization, but SOP $+$ is not coupled at all, for the same reasons that the mode-converting switch of Section VI-B does not couple any light in the bar state. This results in a broadband in-fiber polarizer [38].

Furthermore, tuning mechanisms described in Section VI-A can be employed here to modulate the relative coupling

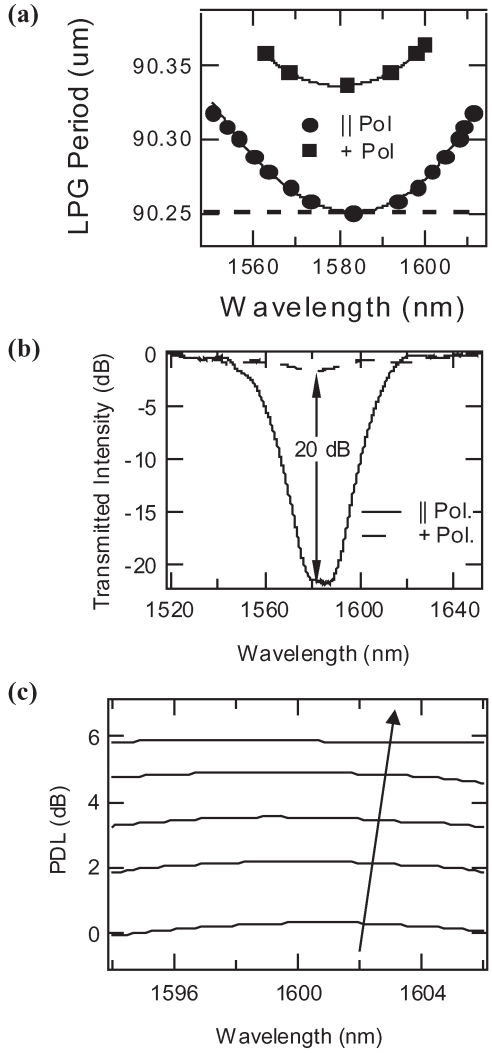

Fig. 23. Polarization-control devices with TAP-LPGs. (a) PMC—separate TAPs for orthogonal SOPs. Horizontal dashed line shows a grating period at TAP for PMC of one of the SOPs. (b) Polarizer grating spectra. 20-dB polarizability at both periods. Device bandwidth is $\sim$ 10 nm. (c) PDL for a 6-dB grating. Continuous tuning from 0 to 6 dB.

efficiencies for the two SOPs of light. The results of strain tuning these gratings (strain range 0–0.05%) are shown in Fig. 23(c). Varying the strain allows the changing of the relative amounts of light attenuated from the two orthogonal polarizations, thus yielding a device whose PDL can be continuously tuned between 0 and 6 dB [39]. While the spectra are only 10-nm wide, fiber dispersion-engineering design rules, described in detail in Section IV-B, can be readily applied to achieve any desired bandwidth.

VIII. Packaging and Stability Considerations

All the devices introduced in this paper utilize the mode-converting capabilities of TAP-LPGs. LPGs are easy to fabricate because the grating periodicities required are of the order of 100 μm, and conventional lithographic tools suffice (i.e., no costly interferometric processes, such as holographic setups or phase masks, are needed). However, LPGs suffer from a high level of sensitivity to environmental and fabrication conditions, such as temperature, humidity, external strain, sensitivity of the PMC to fiber-diameter variations, etc. Thus, while the grating period itself is of the order of 100 μms, the precision required in achieving the desired grating period may be at the submicrometer level. Hence, LPG devices have generally been considered to be costly to manufacture, and even more costly to package, such that their operating responses do not change over time.

TAP-LPG devices differ from conventional LPGs, not only in functionality, as demonstrated in this paper so far, but are also significantly more stable. In addition, the packaging requirements for these gratings are comparable to those of fiber Bragg grating (FBG) devices. This section will address each of the impairments that have been considered debilitating to the commercial deployment of conventional LPG devices and demonstrate how these effects or parameters either have a diminished influence or are cost-effectively manageable in the context of TAP-LPGs.

A. Stability and Reliability of Mode Conversion

The primary distinction between conventional LPGs and TAP-LPGs is in their functionality. While conventional LPGs are used as band-rejection filters, in which light coupled into the HOM (usually a cladding mode of an SMF) is attenuated, TAP-LPG-based devices utilize the HOM for various applications. Thus, while the variation in the residual amount of light left in the fundamental mode is the parameter important for stability considerations in conventional LPGs, the amount of light converted to the HOM is the pertinent parameter in the context of TAP-LPGs. The mode-conversion efficiency η of a uniform LPG of either kind can be expressed as

$$\eta = (\kappa L_{\rm g})^2 \frac{\sin^2(\sqrt{(\kappa L_{\rm g})^2 + (\delta L_{\rm g})^2}}{(\kappa L_{\rm g})^2 + (\delta L_{\rm g})^2} \tag{9}$$

where κ is the coupling efficiency of the grating, which is proportional to the UV-induced index change $\Delta n_{\rm UV}$, and $L_{\rm g}$ and δ are the length of the grating and detuning parameter, respectively, as defined earlier. For a moderately strong conventional LPG that yields a 20-dB attenuation peak, the corresponding coupling efficiency is $\eta = 1 - 10^{(-20/10)} = 99\%$. A 2.5% decrease in coupling efficiency, caused by fluctuations in UV-light dosage or lengthwise nonuniformities in fiber parameters, would decrease the attenuation depth by $\sim$ 5.5 dB. On the other hand, the same change in coupling efficiency would only produce a 0.15-dB change for light in the HOM. Since this is the parameter that is of interest in mode-converting TAP-LPGs, it follows that the same physical phenomena perturb the functional parameter by less than an order of magnitude in TAP-LPGs, in comparison to conventional LPGs. The numbers denoted above, have important consequences for assessing the long-term reliability of mode-converting LPGs. Accelerated aging tests on UV-induced FBGs have shown [40] that a decrease in $\Delta n_{\rm UV}$ of 2.5% may be expected over a 25-year operating lifetime of a device that is constantly exposed to ambient temperatures of 70 °C. This would result in a 5.5-dB change of a 20-dB strong LPG-based

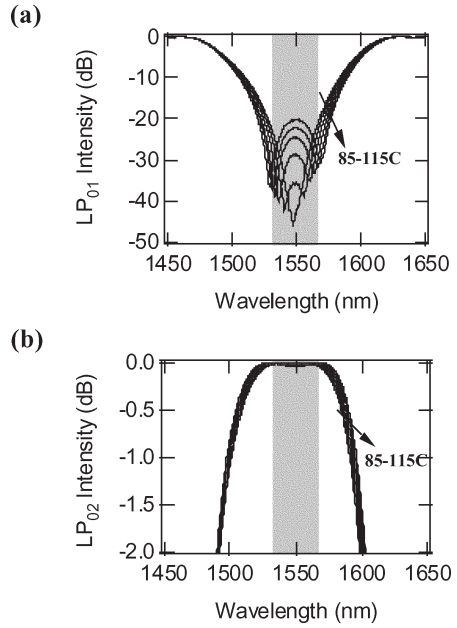

Fig. 24. Response to temperature for both modes of a TAP-LPG. Shaded gray background shows the device operating range (C band). (a) Intensity changes in the LP_{01} mode. (b) Intensity changes in the LP_{02} mode. More than an order of magnitude difference in corresponding intensity changes for the two modes.

band-rejection filter, which would lead to unacceptable long-term performance. Hence, much more stringent thermal-stabilization procedures have traditionally been proposed for conventional LPGs [41]. However, the above analysis shows that mode-converting TAP-LPGs provide more-than-adequate performance, even with a 2.5% change in Δn_{UV}. Thus, it is conceivable that TAP-LPGs can operate in significantly harsher ambient conditions than FBGs.

This difference in behavior is due to the fact that conventional band-rejection LPGs are characterized by the miniscule amount of light that remains in the fundamental mode, and small changes in its intensity would result in large variations on a log (decibel) scale. The relative robustness of the parameter of interest in TAP-LPGs is illustrated in Fig. 24, which shows temperature-dependent spectra of both the modes of a mode-converting grating. Fig. 24(a) shows the spectra for the LP_{01} mode from which light is converted to the desired LP_{02} mode, while Fig. 24(b) shows the corresponding spectra for the LP_{02} mode. The gray backgrounds on the plots are guides to delineate the C-band operating spectral range for the device.

Note that while the intensity value of the LP_{01} mode changes by more than 20 dB, practically no change is observed in the intensity value of the LP_{02} mode for the same temperature swing. This shows that the TAP-LPG mode converters will provide adequate operation even for 30-°C temperature swings. While the data shown in Fig. 24 are for changes in the spectra as a function of temperature, identical behavior is obtained for changes in fabrication parameters (e.g., changes in Δn_{UV}) or other environmental perturbations (e.g., strain). Thus, as a rule, the mode-converting functionality of TAP-LPGs is significantly more robust than the band-rejection functionality of conventional LPGs to manufacturing fluctuations and ambient changes.

B. Polarization Sensitivity and Phase-Matching Tolerance

Practical photonic devices in optical communications networks must have a response that is agnostic to the input SOP of light, because circularly symmetric transmission fibers do not have a preferred SOP for signal propagation. The polarization dependence of mode-converting TAP-LPGs is negligibly small, as already described in Section IV-A. Typically, gratings become more polarization sensitive as their strength increases, since more Δn_{UV} is required for stronger gratings, and saturation of the induced index changes results in an asymmetric index change across the core of a fiber. Experiments described in detail in Section IV-A demonstrate that even the strongest (45-dB strong) mode-converting TAP-LPG shows a polarization dependent change in the LP_{02} mode intensity of less than 2×10^{-4} dB. This miniscule polarization dependence is achieved primarily because both the modes of the fiber are defined by the refractive-index profile of the core, trench, and ring of the fiber (see Fig. 1), and small noncircular perturbations serve to perturb both the modes by similar amounts. Since phase matching with TAP-LPGs is governed by the difference in propagation constants between the two modes, any perturbation that acts on both the modes is invisible to the response of the grating itself.

This factor also makes the fabrication of these gratings more tolerant to small fluctuations in the fiber parameters. Fluctuations, such as lengthwise changes in the dimensions of the fiber or small changes in the refractive-index profile, cause negligible changes to the PMC (see Figs. 3, 5, and 7). Thus, the grating period required for achieving a TAP grating remains relatively constant.

C. Ambient Response

Conventional LPGs also suffer from the fact that the HOM to which coupling occurs is a cladding-guided mode, whose guiding layer is primarily defined by the glass–air interface of an SMF whose outer polymer jacket has been stripped off. Changes at this exposed interface, whether due to water-droplet formation at the glass surface due to ambient humidity, or due to the accidental leakage of fluids on to the fiber surface, will then cause the alteration of the refractive-index profile of the guiding layer that confines the cladding mode. This will result in a shift of the PMC and a corresponding shift in the spectra of conventional LPGs. Thus, hermetically sealing these devices may be necessary in some operating conditions.

However, since the HOM of the few-mode fiber resides in the core, ambient index changes have no effect on the spectra or performance of these devices.

D. Athermal Packaging

Fig. 24 and the associated discussion in Section VIII-A demonstrates that TAP-LPGs are significantly less sensitive to ambient-temperature variations than conventional LPGs. Nevertheless, it reveals that an unpackaged TAP-LPG can operate only over a 30-°C temperature range, which does not suffice for devices deployed in optical networks. The typical operating-temperature range for photonic devices is 60–80 °C. This can

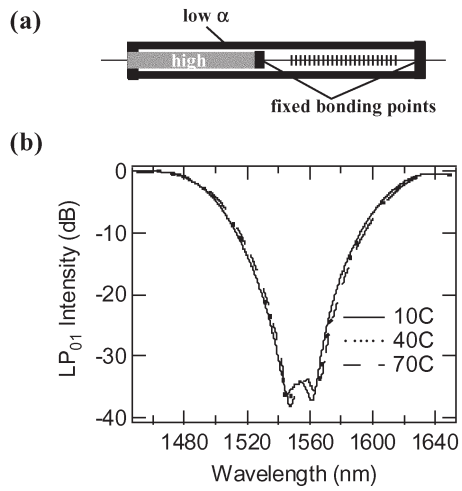

Fig. 25. TAP-LPG packaging for athermal response. (a) Athermal package schematic. Two materials with different CTEs yields negative CTE for composite structure. (b) Resultant temperature-dependent spectra for TAP-LPG. No change in spectrum from 10–70 °C.

be achieved in TAP-LPGs by employing packaging techniques that are commonly used for commercially deployed FBG-based devices [42].

The temperature and strain dependence of TAP-LPGs was described in detail in Section VI-A. Unlike conventional LPGs, the strength, rather than the resonant wavelength of the TAP-LPG, changes when the operating temperature or strain is changed. Note from Figs. 18 and 19 that both temperature and strain cause the TAP-LPG to change in an identical fashion—the strength of the grating increases by 1-dB while maintaining its spectral shape—for a 4 °C temperature increase, as well as a 0.002% strain increase. Thus, a package that releases strain on the LPG by a predetermined amount for a given temperature increase would result in a passively compensated athermal device.

The schematic of the packages used with TAP-LPGs is shown in Fig. 25(a). The package comprises two distinct materials with low and high coefficients of thermal expansion (CTE), respectively, which when assembled in the manner shown in Fig. 25(a), result in a package that has a negative CTE. The negative CTE of the package must satisfy

$$\frac{\mathrm{d}\varepsilon}{\mathrm{d}T} = \frac{\frac{\partial \eta}{\partial T}}{\frac{\partial \eta}{\partial \varepsilon}} \tag{10}$$

where ε is strain, T is temperature, η is the mode-conversion efficiency as defined by (9), and ∂ signifies partial derivates. Fig. 25(b) shows the spectra of a TAP-LPG packaged with the appropriate negative CTE, as a function of temperature. As is evident, the spectra are indistinguishable over a 60 °C range, demonstrating that athermal packages offer an attractive means of obtaining temperature-insensitive performance from TAP-LPGs.

IX. Summary

Few-mode fibers can be designed to possess HOMs with a variety of desired dispersive properties. Coupling between different modes of such fibers with LPGs leads to unique phase-matching phenomena. This enables a variety of active and passive devices for signal-conditioning applications, such as polarization control, spectral shaping, optical filtering, and dispersion control, among others. In addition, the fundamental building block for these devices—the TAP-LPG—is significantly more robust to environmental variations and tolerant of manufacturing variations than conventional LPG devices.

A unique feature of few-mode fiber devices is that it takes the complexity out of the device-fabrication process, and introduces it into the fiber-design process. Dispersion-optimized few-mode fibers can be manufactured using techniques used for transmission fibers. Thus, few-mode fiber devices can potentially be highly cost competitive, since the most complex part of the device (the dispersive fibers) can be mass manufactured.

Acknowledgment

The author would like to thank several researchers and colleagues at Optical Fiber Solutions (OFS) Laboratories, OFS-Fitel, and Bell Laboratories, Lucent Technologies, whose experimental and theoretical contributions were essential for the demonstration and development of many ideas illustrated in this paper. In particular, the contributions of M. F. Yan, E. Monberg, F. V. Dimarcello, J. W. Fleming, L. C. Cowsar, Z. Wang, S. Ghalmi, P. Wisk, D. Peckham, B. Mikkelsen, G. Raybon, and S. Chandrsekhar were critical for results presented in this review.

References

[1] M. J. Li, "Recent progress in fiber dispersion compensators," in *Proc. Eur. Conf. Optical Communication*, Amsterdam, The Netherlands, 2001, pp. 486–489, Paper ThM.1.1.

[2] M. Ibsen, P. Petropoulos, M. N. Zervas, and R. Feced, "Dispersion-free fibre Bragg gratings," in *Proc. Optical Fiber Communication*, Anaheim, CA, 2001, pp. MC1-1–MC1-3.

[3] B. J. Eggleton, A. Ahuja, P. S. Westbrook, J. A. Rogers, P. Kuo, T. N. Nielsen, and B. Mikkelsen, "Integrated tunable fiber gratings for dispersion management in high-bit rate systems," *J. Lightw. Technol.*, vol. 18, no. 10, pp. 1418–1432, Oct. 2000.

[4] A. M. Vengsarkar, P. J. Lemaire, J. B. Judkins, V. Bhatia, T. Erdogan, and J. E. Sipe, "Long-period fiber gratings as band-rejection filters," *J. Lightw. Technol.*, vol. 14, no. 1, pp. 58–65, Jan. 1996.

[5] M. J. Holmes and R. Kashyap, "Side-tap fiber grating filters," presented at the Bragg Gratings, Photosensitivity and Poling Glass, Stuart, FL, 1999, SaC1.

[6] S. H. Yun, B. W. Lee, H. K. Kim, and B. Y. Kim, "Dynamic erbium doped fiber amplifier with automatic gain flattening," in *Proc. Optical Fiber Communication*, San Diego, CA, 1999, pp. PD28/1–PD28/3.

[7] H. Lebidi, J.-J. Guerin, V. Girardon, X. Bonnet, C. Simonneau, R. Boucenna, C. D. Barros, N. Dely, and I. Riant, "Dynamic gain control of optical amplifier using an all-fibre solution," presented at the Eur. Conf. Optical Communication, Copenhagen, Denmark, 2002, Paper PD1.8.

[8] L. Gruner-Nielsen and B. Edvold, "Status and future promises for dispersion compensating fibres," presented at the Eur. Conf. Optical Communication, Copenhagen, Denmark, 2002, Paper 6.1.1.

[9] J.-L. Auguste, R. Jindal, J.-M. Blondy, M. Claeau, J. Marcou, B. Dussardier, G. Monnom, D. B. Ostrowsky, B. P. Pal, and K. Thyagarajan, "−1800 ps/(nm.km) chromatic dispersion at 1.55 μm in dual concentric core fibre," *Electron. Lett.*, vol. 36, no. 20, pp. 1689–1691, Sep. 2000.

[10] C. D. Poole, J. M. Weisenfeld, D. J. DiGiovanni, and A. M. Vengsarkar, "Optical fiber-based dispersion compensation using higher order modes near cutoff," *J. Lightw. Technol.*, vol. 12, no. 10, pp. 1746–1758, Oct. 1994.

[11] T. Erdogan, "Fiber grating spectra," *J. Lightw. Technol.*, vol. 15, no. 8, pp. 1277–1294, Aug. 1997.
[12] X. Shu, L. Zhang, and I. Bennion, "Sensitivity characteristics of long-period fiber gratings," *J. Lightw. Technol.*, vol. 20, no. 2, pp. 255–266, Feb. 2002.
[13] H. J. Patrick, A. D. Kersey, and F. Bucholtz, "Analysis of the response of long period fiber gratings to external index of refraction," *J. Lightw. Technol.*, vol. 16, no. 9, pp. 1606–1612, Sep. 1998.
[14] T. E. Dimmick, G. Kakarantzas, T. A. Birks, A. Diez, and P. S. J. Russell, "Compact all-fiber acoustooptic tunable filters with small bandwidth-length product," *IEEE Photon. Technol. Lett.*, vol. 12, no. 9, pp. 1210–1212, Sep. 2000.
[15] Q. Li, A. A. Au, C.-H. Lin, E. R. Lyons, and H. P. Lee, "An efficient all-fiber variable optical attenuator via acoustooptic mode coupling," *IEEE Photon. Technol. Lett.*, vol. 14, no. 11, pp. 1563–1565, Nov. 2002.
[16] A. Abramov, A. Hale, R. S. Windeler, and T. A. Strasser, "Widely tunable long-period fibre gratings," *Electron. Lett.*, vol. 35, no. 1, pp. 81–82, Jan. 1999.
[17] S. Ramachandran, Z. Wang, and M. F. Yan, "Bandwidth control of long-period grating-based mode converters in few-mode fibers," *Opt. Lett.*, vol. 27, no. 9, pp. 698–700, 2002.
[18] S. Ramachandran, M. Yan, L. Cowsar, A. Carra, P. Wisk, and R. Huff, "Large bandwidth, highly efficient mode coupling using long-period gratings in dispersion tailored fibers," in *Proc. Optical Fiber Communication*, Anaheim, CA, 2001, pp. MC2-1–MC2-3.
[19] S. Ramachandran, M. Yan, E. Monberg, F. Dimarcello, P. Wisk, and S. Ghalmi, "Record bandwidth, spectrally flat coupling with microbend gratings in dispersion-tailored fibers," *IEEE Photon. Technol. Lett.*, vol. 15, no. 11, pp. 1561–1563, Nov. 2003.
[20] S. Ramachandran, M. F. Yan, S. Golowich, E. Monberg, F. V. Dimarcello, J. Fleming, S. Ghalmi, and P. Wisk, "A novel fiber design for polarisation insensitive microbend gratings," presented at the Eur. Conf. Optical Communication, Stockholm, Sweden, 2004, Paper Th2.3.2.
[21] C. D. Pool, C. D. Townsend, and K. T. Nelson, "Helical-grating two-mode fiber spatial-mode coupler," *J. Lightw. Technol.*, vol. 9, no. 5, pp. 598–604, May 1991.
[22] S. Savin, M. J. F. Digonnet, G. S. Kino, and H. J. Shaw, "Tunable mechanically induced long period fiber gratings," *Opt. Lett.*, vol. 25, no. 10, pp. 710–712, 2000.
[23] M. Wandel, T. Veng, Q. Le, and L. Grüner-Nielsen, "Dispersion compensating fibre with a high figure of merit," in *Proc. Eur. Conf. Optical Communication*, Amsterdam, The Netherlands, 2001, pp. 52–53, Paper PD-A.1.4.
[24] K. Oh, H. S. Seo, J. K. Lee, and U. C. Paek, "Polarization dependent dispersion characteristics of higher order modes in cylindrical dual mode fiber with an arbitrary index profile," *Opt. Commun.*, vol. 159, no. 1–3, pp. 139–148, 1999.
[25] C. D. Poole, J. M. Wiesenfeld, and D. J. Digiovanni, "Elliptical-core dual-mode fiber dispersion compensator," *IEEE Photon. Technol. Lett.*, vol. 5, no. 2, pp. 194–197, Feb. 1993.
[26] M. Eguchi, M. Koshiba, and Y. Tsujji, "Dispersion compensation based on dual-mode optical fiber with inhomogeneous profile core," *J. Lightw. Technol.*, vol. 14, no. 10, pp. 2387–2394, Oct. 1996.
[27] S. Ramachandran, B. Mikkelsen, L. C. Cowsar, M. F. Yan, G. Raybon, L. Boivin, M. Fishteyn, W. A. Reed, P. Wisk, D. Brownlow, R. G. Huff, and L. Gruner-Nielsen, "All-fiber, grating-based, higher-order-mode dispersion compensator for broadband compensation and 1000-km transmission at 40 Gb/s," *IEEE Photon. Technol. Lett.*, vol. 13, no. 6, pp. 632–634, Jun. 2001.
[28] A. H. Gnauck, L. D. Garrett, Y. Danziger, U. Levy, and M. Tur, "Dispersion and dispersion-slope compensation of NZDSF over the entire C band using higher order mode fibre," *Electron. Lett.*, vol. 36, no. 23, pp. 1946–1947, Nov. 2000.
[29] S. Ghalmi, S. Ramachandran, E. Monberg, Z. Wang, M. F. Yan, F. V. Dimarcello, W. A. Reed, P. Wisk, and J. Fleming, "Low loss, all-fiber high-order mode dispersion compensators for lumped or multi-span compensation," *Electron. Lett.*, vol. 38, no. 24, pp. 1507–1508, Nov. 2002.
[30] J. L. Gimlett and N. K. Cheung, "Effects of phase-to-intensity noise conversion by multiple reflections on gigabit-per-second DFB laser transmission systems," *J. Lightw. Technol.*, vol. 7, no. 6, p. 888, Jun. 1989.
[31] S. Ramachandran, S. Ghalmi, J. Bromage, S. Chandrasekhar, and L. L. Buhl, "Evolution and systems impact of coherent distributed multi-path interference," *IEEE Photon. Technol. Lett.*, vol. 17, no. 1, pp. 238–240, Jan. 2005.
[32] M. Tur, E. Herman, A. Kozhekin, and Y. Danziger, "Stimulated brillouin scattering in high-order-mode fibers employed in dispersion management modules," *IEEE Photon. Technol. Lett.*, vol. 14, no. 9, pp. 1282–1284, Sep. 2002.
[33] S. Ramachandran, B. Mikkelsen, L. C. Cowsar, M. F. Yan, G. Raybon, L. Boivin, M. Fishteyn, W. A. Reed, P. Wisk, D. Brownlow, R. G. Huff, and L. Gruner-Nielsen, "All-fiber, grating-based, higher-order-mode dispersion compensator for broadband compensation and 1000-km transmission at 40 Gb/s," presented at the Eur. Conf. Optical Communication, Munich, Germany, 2000, Paper PD-2.5.
[34] S. Ramachandran, G. Raybon, B. Mikkelsen, M. F. Yan, L. Cowsar, and R.-J. Essiambre, "1700-km transmission at 40-Gb/s with 100-km amplifier-spacing enabled by higher-order-mode dispersion-compensation," *Electron. Lett.*, vol. 37, no. 22, pp. 1352–1354, Oct. 2001.
[35] S. Ramachandran, S. Ghalmi, Z. Wang, and M. Yan, "Band-selection filters with concatenated long-period gratings in few-mode fibers," *Opt. Lett.*, vol. 27, no. 19, pp. 1678–1680, 2002.
[36] D. S. Starodubov, V. Grubsky, and J. Feinberg, "All-fiber bandpass filter with adjustable transmission using cladding-mode coupling," *IEEE Photon. Technol. Lett.*, vol. 10, no. 11, pp. 1590–1592, Nov. 1998.
[37] S. Ramachandran, S. Ghalmi, S. Chandrasekhar, I. Ryazansky, M. Yan, F. Dimarcello, W. Reed, and P. Wisk, "Tunable dispersion compensators utilizing higher order mode fibers," *IEEE Photon. Technol. Lett.*, vol. 15, no. 5, pp. 727–729, May 2003.
[38] S. Ramachandran, M. Das, Z. Wang, J. Fleming, and M. Yan, "High extinction, broadband polarisers using long-period fiber-gratings in few-mode fibers," *Electron. Lett.*, vol. 38, no. 22, pp. 1327–1328, Oct. 2002.
[39] M. Das, S. Ramachandran, Z. Wang, J. Fleming, and M. Yan, "Broadband, adjustable polarisation-dependent-loss compensators with long-period fiber-gratings," presented at the Eur. Conf. Optical Communication, Copenhagen, Denmark, 2002, Paper 10.4.5.
[40] S. Kannan, J. Z. Y. Guo, and P. J. Lemaire, "Thermal stability analysis of UV-induced fiber Bragg gratings," *J. Lightw. Technol.*, vol. 15, no. 8, pp. 1478–1483, Aug. 1997.
[41] S. Kannan, L. Copeland, J. Judkins, M. LuValle, and P. J. Lemaire, "Reliability of long-period gratings," in *Proc. Optical Fiber Communication*, San Jose, CA, 1998, pp. 282–283, ThG6.
[42] W. W. Morey and W. L. Glomb, "Incorporated Bragg filter temperature compensated optical wavelength device," U.S. Patent 5 042 898, Aug. 27, 1991.

Siddharth Ramachandran (M'99) received the Bachelor of Technology degree from the Indian Institute of Technology, Kanpur, in 1991, the M.S. degree from the University of Wisconsin, Madison, in 1993, and the Ph.D. degree in electrical engineering from the University of Illinois, Urbana, in 1998.

His graduate work focused on the optical properties of chalcogenide glasses. Since November 1998, he has worked at Bell Laboratories, Lucent Technologies and subsequently OFS Laboratories, OFS-Fitel, Somerset, NJ, first as a Member of Technical Staff and, since March 2003, as a Distinguished Member of Technical Staff. His research focuses on investigating fiber and fiber-grating devices in specialty dispersion-tailored fibers. He has authored 72 refereed journal and conference publications, two book-chapters, 12 patent applications, and is the editor of an upcoming Springer-Verlag book on fiber-based dispersion compensation.

Dr. Ramachandran is a member of IEEE-LEOS.